Energy & Buildings 315 (2024) 114293

Contents lists available at ScienceDirect

Energy & Buildings

journal homepage: www.elsevier.com/locate/enbuild

Futures for electrochromic windows on high performance houses in arid, cold climates

Daniel L. Villa [a,*], Nathan T. Hahn [a], John K. Grey [a], Frances Pavich [b]

[a] Sandia National Laboratories, P.O. Box 5800 MS 0710, Albuquerque, 87185-0710, NM, United States
[b] Transcendence LLC, 21 Vista Valle Circle, Santa Fe, 87540, NM, United States

ARTICLE INFO

Keywords:
Electrochromic windows
Building energy modeling
Energy efficiency
Climate change
Thermal resilience
Passive house

ABSTRACT

This study investigates high performance electrochromic windows used on a passive house and residential dwelling to IECC 2021 (i.e., IECC dwelling). In the lab, the electrochromic film switches transmitted solar heat gain coefficient (SHGC) from 0.09 to 0.7 and visible transmittance from 0.15 to 0.82 with power consumption of 1.23 W/m^2 during switching times less than 3 minutes. We extrapolate these results to a window assembly. Building energy models of the houses were evaluated in Santa Fe, New Mexico. A Monte Carlo analysis for 2020, 2040, 2060, and 2080 was conducted for Shared Socioeconomic Pathways 2-4.5, 3-7.0, and 5-8.5. Cases with and without the electrochromic windows and with and without electricity were used to determine energy use intensity and hours beyond thermal safety thresholds.

The passive house showed 1.3-3.1% mean energy savings and the IECC dwelling 4.4-5.1% with electrochromic efficiency benefits growing into the future for both cases. Even so, overall savings decrease into the future for the passive house, due to growth in cooling load being dominant, conversely overall energy savings increase into the future for the IECC dwelling due to heating loads being dominant. For thermal resilience, the passive house exhibited a mean percent decrease of 0.02-0.31% hours in the extreme caution (i.e., > 32.2 °C, ≤ 39.4 °C) range while the IECC dwelling exhibited 0.38-4.38%. The study therefore shows that electrochromic windows will have smaller benefits for the passive house in comparison to the IECC dwelling. The relationship between electrochromic windows is shown to have a complex relationship between house efficiency and climate change by these results.

1. Introduction

1.1. Background

Human society must mitigate most anthropogenic green house gas (GHG) emissions to keep global average temperature anomaly from exceeding 2 °C [1]. It is also important to assure that human society can adapt to new extreme climate conditions. Such adaptations can become "maladaptations" [2] when they protect humanity but accelerate climate change by increased GHG. Extreme heat is the most certain threat to humanity from global warming. It is well established that heat waves (HWs) are increasing in frequency duration and intensity [3–5]. It is estimated that trillions of United States (U.S.) dollars are being lost globally due to extreme heat with disadvantaged individuals taking the greater losses [6]. In addition to extreme heat, extreme cold may also be increasing in intensity even though average conditions are warmer [7,8]. Energy efficiency (EE) and safety during extreme heat or cold (i.e., "thermal resilience") are therefore pressing issues in humanity's future.

Buildings are the primary means by which humanity shelters from extreme temperature conditions. They are also a primary contributor to GHG emissions. In 2019, buildings represented 38% of global GHG emissions with 11% being materials for new construction [9]. The buildings sector is therefore at the forefront in the process of adapting to extreme temperatures and mitigating GHGs. Unfortunately, growth in new construction and demand for air conditioning have proven to be a "maladaptation" [2]. According to the United Nations Environment Programme, building emissions peaked in 2021 at 10 $GtCO_2$ which was an increase of 5% from 2020. Buildings consumed 34% of global energy which increased 4% from 2020 despite significant investment in EE [10]. Such a trajectory is creating a growing gap between 2050 net-zero goals and reality. Inefficient buildings must therefore be phased

* Corresponding author.
E-mail address: dlvilla@sandia.gov (D.L. Villa).

https://doi.org/10.1016/j.enbuild.2024.114293
Received 23 January 2024; Received in revised form 8 April 2024; Accepted 12 May 2024
Available online 16 May 2024
0378-7788/© 2024 The Author(s). Published by Elsevier B.V. This is an open access article under the CC BY license (http://creativecommons.org/licenses/by/4.0/).

out in the coming decades through retrofits to existing buildings and by efficient new construction.

One important part of making buildings more efficient is through the use of advanced window technologies. The current window stock in the U.S. represents 10% of total building energy use [11]. This can be cut in half by smart window technologies that adapt their properties to provide EE benefits. Wholesale adoption of smart windows has potential for 2-3% reduction of U.S. GHG. Cost has been a primary barrier to smart window technology adoption though [11]. The lowest costs we found for smart windows was \$61/ft^2 installed [12]. One vendor lists prices as \$85-135/ft^2 installed with their switching films costing \$25-45/ft^2 [13]. This is much higher than triple pane windows that cost \$25 to \$40/ft^2 installed [14]. Even so, economic analyses have shown that the up-front higher cost can lead to a good return on investment but results often have a long payback period or are not cost-effective [15–17]. Though we do not address cost in this study, there is potential for reducing cost in the materials and processing techniques used to produce the high performance electrochromic windows (ECWs) we analyze.

1.2. Electrochromic windows

ECWs use reversal of an electric potential to move ions such that an Electrochromic (EChr) film transitions from transparent to opaque [18]. Good films can switch states with low power for many cycles. This is advantageous for many reasons including control of lighting, privacy, and EE applications. The EChr film inspiring this study is made of poly(diphenylamine) that has potential for significant reductions in film costs (i.e., it does not require vacuum-based deposition to form metal-oxide films) [19]. In addition, the film is higher performance than current films on the market. High values for $\Delta SHGC$ are 0.38 with most products spanning between 0.25 and 0.37 and for ΔVT the largest span was 0.67 with most falling between 0.4 and 0.55 (see section 2.3 of [20]). In the lab, the material analyzed here can switch transmitted SHGC from 0.09 to 0.7 as visible transmittance (VT) varies from 0.15 to 0.82. Based on the operating voltage and current, a window based on this film would require on average 1.23 W/m^2 for switch times of 3 minutes. So far, the measurements are only for small samples though and further development is needed to apply these to an entire window assembly. Also the change in SHGC is only for the transmitted term and the absorbing term still needs to be measured. Finally, these results are only for room temperature. There are many factors that could drive performance to a better state than current results, but losses from integration into a stack of materials and other constraints will also reduce this performance.

We therefore analyze a case that extrapolates the lab results for transmitted SHGC to total SHGC to estimate EE and thermal resilience potential. Though temperature dependence will be present (e.g., see [21] for comparable material investigations), we assume no effect. The truth of this assumption will depend on the design of the ECW assembly. Regardless, the first results for these polymeric films indicate that three of the U.S. Department of Energy goals for smart windows [11] (i.e., $\Delta SHGC \geq 0.6$, switching time < 3 min, Switching power ≤ 3 W/m^2) are likely to be achieved by these or similar materials at lower costs. The Department of Energy goals for state maintenance (≤ 72 Wh/m^2/day) and cycling durability ($\geq$ 50,000 cycles per ASTM 2141) have not yet been measured for our film.

1.3. High performance houses

Windows can only save energy in comparison to houses with no windows under well-designed circumstances. Windows can admit solar radiation as a free source of heating. There is a penalty though when cooling is needed. ECWs can partially overcome this issue by decreasing SHGC when heat is not needed. Windows can also save energy through daylighting since less electric lighting is needed. Finally, if more reflective than the envelope, windows can reflect more energy away when cooling is needed. Beyond these three effects, windows are detrimental to EE because they seldom provide as much insulation as the rest of the envelope. Regardless, windows are retained under such circumstances for aesthetic reasons.

High performance houses and increasingly efficient light-emitting diodes are raising the number of cases where windows are detrimental to EE. An estimate of a threshold where windows cannot provide EE benefits, C_w, (with latent and radiation loads assumed to be negligible) is the night-time ratio of thermal loads not associated with space heating (i.e. plug loads, human heat release, etc.) to heat losses from the structure during winter. When C_w is greater than 1, heat is never needed and adding extra heat through a window cannot benefit EE:

$$C_w = \frac{Q_{in}}{U_g A_g \left(T_{in} - T_g\right) + U_{out} A_{out} \left(T_{in} - T_{out}\right) + Q_{inf} + Q_{vent}} > 1 \qquad (1)$$

Here Q_{in} is the average internal heat load during the winter in the absence of space heating. The terms U_g and U_{out} are the average ground slab and average above ground heat transfer coefficients. The terms A_g and A_{out} are the corresponding surface areas. The terms T_{in}, T_{out}, and T_g are the average thermostat temperature during night for the winter, average night-time winter ambient temperature, and average near-surface ground temperature. The terms Q_{inf} and Q_{vent} represent heat transfer due to infiltration and ventilation.

This ratio, C_w is dependent on both climate and house envelope. When greater than one, the ratio certainly indicates that windows will not save energy. Values less than one may also not save energy because of cooling losses in the summertime. Increases in building envelope efficiency will lead to reductions in the heat transfer coefficients in equation (1). Also, increases in the temperature terms besides T_{in} will continue into the future because of climate change. This implies that windows will be increasingly inefficient in larger geographical areas in the future.

We therefore analyze ECWs applied to two house designs. The first is a passive house (PH) design for which C_w is much closer to one than most other houses such that only a small amount of heating is needed. This design is feasible with current technology and is typical to passive house standards [22,23]. The second is high efficiency but still requires a larger heating load due to less insulation. We use the U.S. Department of Energy residential single dwelling house per the International Energy Conservation Code (IECC) 2021 [24] residential standard (i.e., the “IECC dwelling” in the rest of the paper). We make this comparison to quantify how benefits of ECWs vary for future climates at two different points near the C_w threshold.

We analyze the EE and thermal resilience benefits of ECWs via 4 configurations of each of the PH and IECC dwelling. The configurations are: 1) with ECWs, 2) without ECWs 3) with ECWs and no electricity, and 4) without ECWs and without electricity. This enables the study to show how energy savings and thermal resilience are related between active and nearly passive performance (i.e., with a small amount of backup power for EChr switching and ventilation).

1.4. Santa Fe’s climate

We use the city of Santa Fe, New Mexico in the U.S. as a case study. Santa Fe has a cold, sunny, high-desert climate (Climate Zone 5B [25]) with historic averages of 3,500 °C·day heating degree days, 220 °C·day cooling degree days, and average precipitation 0.37 m/yr [26]. Though this is ideal for saving energy with windows through solar passive design [27], the C_w threshold for the PH and high efficiency heat pumps can make windows purely a detriment to EE in Santa Fe. Climate warming will make this more the case for the future. The range of outcomes for Santa Fe’s future climate decrease heating degree days by 330-1,800 °C·day and increase cooling degree days by 110-1,400 °C·day by the year 2100 depending on climate scenario [26]. Precipitation is expected to slightly decrease.

1.5. Future weather approach

The effects future extreme temperatures will have on high performance houses with ECWs around the C_w transition has not been sufficiently investigated. We analyze future conditions including extreme heat and extreme cold conditions using the multiscenario extreme weather simulator (MEWS) [28]. MEWS is a stochastic generator of future HWs and cold snaps (CSs). It uses U.S. National Oceanic Atmospheric Administration (NOAA) climate normals and 50 years or more of NOAA daily summaries to baseline to current conditions. It then amplifies the frequency and intensity in comparison to the current conditions based on Intergovernmental Panel on Climate Change (IPCC) data [29]. The output is a set of HW and CS events that can be interposed over typical conditions to form an hourly time series that has new extreme temperature events added to it. The stochastic generator can be used to generate enough files to perform a Monte Carlo study.

1.6. Research questions

This study is motivated by the desire to show how ECWs affect high performance housing in the present and future. The context of the following research questions is for Santa Fe's climate in both present (i.e., 2020) and future conditions (i.e., 2040, 2060, and 2080) over three shared socioeconomic pathways (SSPs) [30]:

- How much energy can ECWs save for a PH design in comparison to efficient code-compliant construction?
- If only ECWs and smart ventilation remain operational, How much better thermal resilience does the PH design exhibit than the efficient code-compliant construction?

The idea behind the second research question is to show whether ECWs and smart ventilation with small power load profiles can make a big difference for thermal resilience. Under such conditions, a small amount of backup power can make a large difference in thermal resilience.

1.7. Outline

This paper provides a brief literature review that shows current work on smart windows in buildings and building energy model (BEM) studies on energy savings. It then provides an in-depth description of the methods used. This starts with the characteristics of the EChr film being analyzed. It then describes the BEM and automatic scripting used to add ECWs, solar hot water, and smart ventilation. This is followed by specification of the MEWS analysis. The methods section ends with description of the metrics used in the study. The results section gives data from the MEWS analysis. It then provides tables and figures that show EE and energy consumption of the ECWs for present and future conditions with confidence intervals for each SSP. The results section ends with provision of similar information for thermal resilience for extreme hot and extreme cold conditions. The discussion section then elaborates how the highly efficient models analyzed have less EE savings than most cases in the literature. Difficulties in the MEWS analysis are also discussed. The paper finishes with giving some conclusions and suggests future work.

2. Literature review

ECW technologies were developed over 50 years ago [31]. The increased urgency for EE due to climate change has made smart window technologies research grow to a vast field. Here, we focus on applications applied to building energy modeling and climate change. Many reviews of competing technology types of smart windows including EChr [32–35], thermochromic [36–39], photochromic [40], super capacitor materials [41], other responses (e.g., humidity, physical force, magnetism etc.) [42,43], and liquid crystal materials [44]. General reviews of competing approaches are also available [45,46].

Though the literature of modeling and experimental studies for smart windows is extensive (e.g., [47,48,20,49,50]), most are focused on how present performance can help mitigate climate change. No studies we could find have assessed how future conditions will affect both EE and thermal resilience of residential buildings with no electric power from the grid but with operative ECWs. Even so, it is well established that climate zone affects what smart window technologies are the most effective. Variation across climate zones therefore gives a sense of how future warmer conditions will affect smart window performance. Rashidzadeh et al. show the complexity of different outcomes for different climate zones with extensive maps [51]. Fathi and Kavoosi analyze several climate zones in Iran and conclude that for high-rise office buildings EChr and integrated photovoltaics were most effective at higher latitudes and saved up to 35% energy. Such large savings are mainly driven by the 85% window to wall ratio (WWR) used by Fathi and Kavoosi. In such conditions ECWs become blockers of excessive solar heat while letting some of it in when needed. Fekri et al. are closer to our study and investigated residential buildings with smart windows in several climate zones across the U.S. including a case in New Mexico. Their work found that climates with larger variations in temperature led to heating ventilation and air conditioning (HVAC) energy savings ranging from 8.6% in Honolulu (very little seasonal variation) to maximum savings in New Mexico of 26.7%. Their work does not look at how New Mexico's future climate will affect such results though [52]. In juxtaposition, Hoon Lee et al. analyzed ECWs across six climate zones for a commercial building with WWR of 0.33 and found less HVAC energy savings for Denver (9.75%) and colder climates than hotter climates like Miami (13.46%) [53]. This shows that EE outcomes for ECWs are complex and dependent on climate and building characteristics.

The only other study we have found that looks at how smart windows will perform in future climates is from De Masi et al. who performed a combined experimental and simulation based look at a liquid crystal technology and then project it to 2050 and 2080 [54]. The Mediterranean climate analyzed is significantly warmer, the smart glass much lower performance, and the model setup was geared toward experimental validation. This study was therefore not well suited to compare to our PH assessment.

We conclude our review stating that our investigation is a unique computational study of an envisioned state-of-the-art EChr glazing applied to PH and the IECC dwelling for future conditions in Santa Fe. Answers to our research questions therefore make a new contribution to the literature.

3. Method

We first introduce the EChr film followed by the BEM modeling. We then discuss how controls work for the ECWs, smart ventilation, and solar hot water implemented in the PH. This is followed by description of the MEWS case study in Santa Fe and specification of the EE and thermal resilience metrics used.

3.1. Electrochromic material lab testing

Details of the synthesis and performance of the exemplar EChr polymer films considered in this study are described by Grewal et al. [19]. Briefly, the films consist of p-type poly(diphenylamine) doped with poly(4-styrene sulfonate) electrodeposited onto indium-tin-oxide coated glass slides. Transmittance spectra were measured in a non-aqueous electrolyte from 300 to 1800 nm wavelengths under applied biases ranging from -0.1 to 0.95 V (vs. Ag/AgCl). These measurements were used to calculate the transmitted SHGC of their lightened and darkened states, respectively. The transmitted SHGC was found to vary from 0.09 to 0.70 while the VT varied from 0.15 to 0.82.

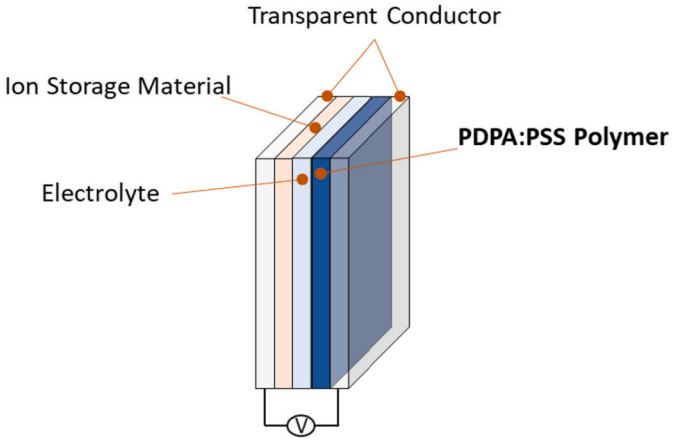

Fig. 1. EChr poly(diphenylamine):poly(4-styrene sulfonate) film layers description. A voltage is applied across the transparent conductors to move ions into and out of the ion storage material. The layers shown here must be assembled into a conventional window assembly with additional layers that address light, color, and protection of the film.

Power consumption for a target device switching time of 3 minutes was calculated based on the film operating voltage, capacity, and several device-specific assumptions. An example of a complete device is shown in Fig. 1, in which the poly(diphenylamine):poly(4-styrene sulfonate) polymer comprises the primary EChr layer. The polymer films require only 19 mC/cm^2 of charge to fully switch, corresponding to an average current density of 0.11 mA/cm^2. The average voltage of the projected device during switching was approximated as:

$$V_{dev} = E_{film} - E_{counter} + I R \quad (2)$$

where E_{film} is the film redox potential (-0.1 V for lightening, 0.95 V for darkening), $E_{counter}$ is a predicted counter electrode potential (assumed as -0.5 V vs. Ag/AgCl based on initial testing), I is the current, and R is the overall device resistance (assumed as 100 Ω). These assumptions yield an average V_{dev} of 1.14 V and power consumption of 1.23 W/m^2 for 3 min switching.

Although these calculations can only be taken as rough estimates, they provide a reasonable basis from which to model ECW impacts on house energy savings. The SHGC and VT were used directly in EnergyPlus as estimates for a window assembly's total integrated SHGC and VT.

For comparison to current market performance, an "on the market" case is also analyzed for TMY version X (TMYx) 2007-2021 weather only [55]. No change to U-value was made but SHGC and VT on the high side were changed to 0.46 and 0.51 respectively. This is representative of current on the market ECWs [20].

3.2. EnergyPlus models

The two EnergyPlus models analyzed in this study are shown in Fig. 2 with the PH on the left and the IECC dwelling model on the right. Table 1 provides an overview of the model properties for both models. The IECC dwelling has about one half of the insulation levels of the PH design. Both designs have low-e windows with triple pane glass for the PH and double pane glass for the IECC dwelling. As can be seen from Figure 2, the PH design has nearly twice the floor space even though it is only a single story dwelling. The PH south facing glass has been adjusted to receive the correct amount of heat to minimize need for HVAC when ECWs are used. It also has good shading on the east and west sides with optimal shading for summer winter variation on the sourthern windows for Santa Fe [27]. The air infiltration leakage rate seen in Table 1 assumes well-built stuctures with leakage rates that are one-twentieth of a 50 Pa air blower test with 0.6 air changes per hour. This leads to 0.0375 air changes per hour average leakage [56]. This represents very well sealed structures for both cases that meets the Passive House Institute's requirements [22]. The PH uses more than double the plug loads than the U.S. national average for single family detached homes in the Midwest of 4,530 kWh/yr [57]. This is intended to indicate that the house is used intensively with higher use on water sanitation and air purification than is typical.

The high-performance PH design whose target total site energy use intensity (EUI) of less than 50 kWh/m^2/yr is well below the Passive House Institute and PassiveHaus requirements that primary energy be less than 120 kWh/m^2/yr and 135 kWh/m^2/yr respectively [58,23]. All energy used by the building will be met by renewable energy and battery storage making site energy nearly equivalent to primary energy. The PH design uses exceptionally high-end EE measures with above average plug load use and with ample lighting to keep conditions well lit when ECWs switch to very low visible transmission levels of 0.15 to block heat. The model contains six thermal zones including an entry way and front living room with 5.57 m tall vaulted ceiling and clerestory southern facing windows to allow solar heat to enter the northern front entry way. The model includes 6 thermal zones seen in Fig. 3 representing 1) Unconditioned garage with heat pump water heater, washer, dryer, and 2nd refrigerator in it, 2) Formal dining, entry, and living area 3) Northeast bedroom 4) Master bedroom 5) Den and kitchen, and 6) Southeast bedroom. Three thick concrete walls (0.35 m) that add 21.2 kWh/K provide additional thermal mass for the PH design. Special guidance for Santa Fe was used in the development of the design [27]. Though the design is very high efficiency, it is not optimal. The presence of windows leads to losses because the C_w value of 0.51 seen in Table 1 and high efficiency heating make the thermal losses through the windows dominant. Windows are still used for aesthetic reasons and ECWs enhance the performance of this non-optimal design.

The IECC dwelling model has several updates to reflect a high EE home that was built to IECC 2021 code standards (i.e., "IECC dwelling") [24]. IECC 2021 has a large difference in comparison to IECC 2018 with increased R-value from 49 (2018) to 60 for ceilings, required continuous insulation with R-value 5 or greater in all walls beyond standard insulation, and twice as deep slab continuous insulation with R-value of 10. The standard has tighter requirements for windows with U-value of 1.70 W/m2/K in comparison to 1.82 W/m2/K. It also requires higher envelope tightness [59]. Updating through retrofits from IECC 2015 to IECC 2021 in New Mexico has an average life cycle cost savings of 4,191 U.S. dollars with 12% first year energy cost savings [60]. This shows that both new construction and existing construction retrofits are economically favorable when upgrading to IECC 2021 in New Mexico. IECC 2021 is available at no cost online [24]. As seen in Figure 3, the IECC dwelling model is composed of only two thermal zones with the entire area of both floors being a single conditioned thermal zone and the attic being the second unconditioned zone.

Four configurations of each model were created leading to a total of eight BEMs:

1. Baseline (BL) case (just described)
2. BL no electricity (NE) (i.e., heating, lighting, plug loads, and cooling are deactivated in EnergyPlus)
3. ECW (see section 3.1 for SHGC and VT, Table 1 for U-value, and section 3.3.1 for controls method)
4. ECW NE

It was assumed that both the smart ventilation and ECWs remain active even with NE.

All models were created and adjusted in the Open Studio^{TM} software development kit 3.5.1 and graphical user interface version 1.5.1 [61,62] and SketchUp^{TM} Pro 2021 version 21.1.332 with the Open Studio Plug in version 1.4.0.

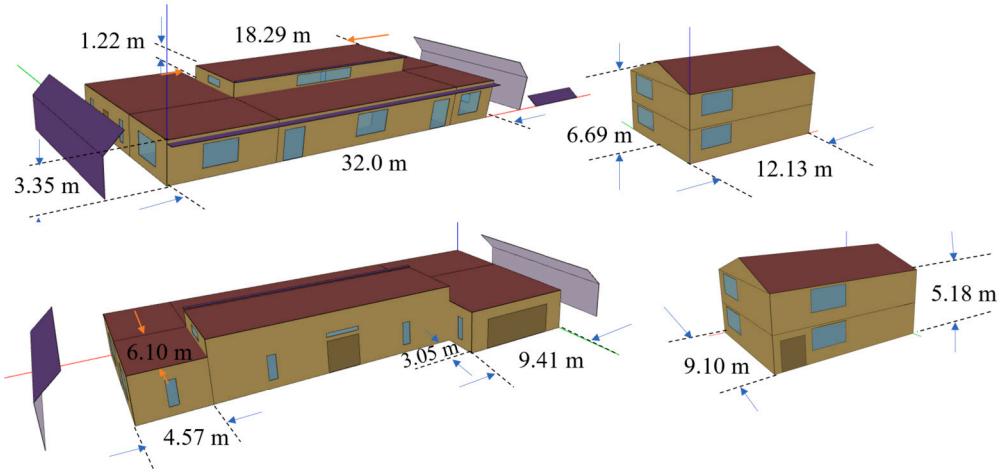

Fig. 2. PH (left) and IECC dwelling (right) model dimensions. The sizes are roughly to scale. A southwest view is shown in the upper figures and a northeast view is shown in the lower ones.

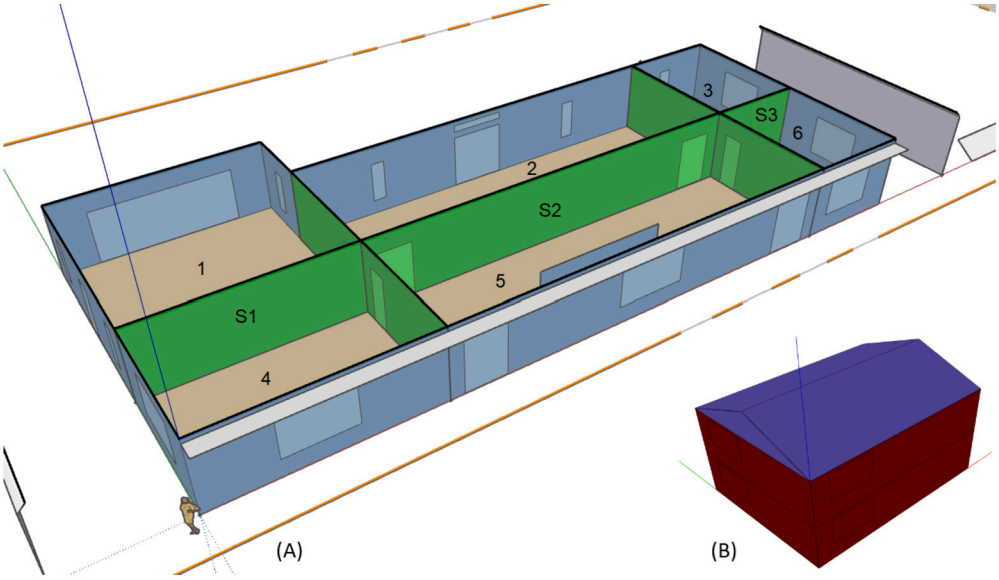

Fig. 3. (A) PH interior thermal zones (green represents shared heat transfer surfaces while blue shows surfaces touching exterior air and tan ground contact. White surfaces are shading surfaces including a part of the solar hot water system on the far right). Shown are: 1) Garage 2) Entry way, 3) Northeast bedroom, 4) Master bedroom, 5) Kitchen/Den, and 6) Southeast bedroom. S1, S2, and S3 are all 0.35 m thick concrete walls for thermal mass. (B) IECC dwelling model living area (dark red) and attic (purple) thermal zones. (For interpretation of the colors in the figure(s), the reader is referred to the web version of this article.)

3.3. Open studio measures

Three Open Studio measures [65] were created to simulate the ECWs, smart ventilation, and solar hot water systems. We use EnergyPlus energy management system programs to control all three systems [66].

3.3.1. Electrochromic window control

The model used for ECWs is similar to Dutta's approach using the EnergyPlus energy management system features to switch between window tint states [67]. Our approach only uses two tint states though to either block or admit heat. Instantaneous switching is assumed since the transition switch time is faster than the 15 min EnergyPlus time step. The ECWs are controlled for each zone [66]. If the mean radiant temperature within that zone is above a setpoint, then the windows are switched to minimize incoming heat. Alternatively, if the mean radiant temperature falls below the same setpoint, then the windows are switched to maximize incoming heat. For this study, the mean radiant temperature setpoint was set to 25 °C which is elevated by 2.5 °C from normal comfort conditions per section 5.3.1.2.1 of [68].

3.3.2. Smart ventilation

The smart ventilation design opens strategically placed intake and outtake vents using automated actuators. A fan near the ground then pulls air through a minimum efficiency reporting value (MERV) 13 filter [69]. Air exits through a roof level vent taking advantage of the thermal stack effect. The intakes include actuators that seal well when closing so that leakage does not occur. The actuators are controlled for economization as follows: 1) If heating is needed and outside dry bulb temperature is hotter than the zone air temperature, open vents and turn on the fan. Otherwise keep the vents closed and the fan off. 2) If cooling is needed and outside dry bulb temperature is colder than the zone air temperature, open vents and turn on the fan. Otherwise keep the vents closed and the fan off. For each zone, inputs of fan pressure rise of 100 Pa (typical for a 0.6 x 0.6 m MERV 13 filter at the flow rates required [70,71,69]) with fan efficiency of 0.8 were given. The flow

Table 1
Summary building inputs for models without ECWs. For detailed inputs, the models are available at [84]. Requests can also be made to the corresponding author.

Model Attribute	PH	IECC Dwelling
Envelope		
Levels	1	2
Number of Occupants	5	3
Roof Geometry	Flat	Pitched
Floor Area (m^2)	418.1	220.8
Total Volume (m^3)	1538	580.3
Conditioned Floor Area (m^2)	334.5	220.8
Roof RSI (m^2 K/W)	10.97	5.53
Walls RSI (m^2 K/W)	8.70	3.53
Floor RSI (m^2 K/W)	3.70	3.53
Window SHGC	0.34	
Window VT	0.88	
Window U-value (W/m^2/K)	0.90	1.70
North WWR	2.98	13.12
East WWR	17.77	15.28
South WWR	22.65	13.12
West WWR	14.48	15.28
Window glass area (m^2)	52.31	32.98
Constant Infiltration Leak Rate (air changes per hour)	0.0375	
Thermally Independent Electric Loads		
Lighting (kWh/m^2/yr)	7.76	4.70
Plug Loads ((kWh/m^2/yr))	24.33	35.82
External Lighting ((kWh/m^2/yr))	0.84	0.96
C_w (see equation (1))	0.51	0.20
Thermally Dependent Electric Loads		
Hot Water	Solar hot water with heat pump water heater backup in garage	Heat pump water heater in attic
HVAC	Ductless water source heat pump in each thermal zone with ground heat exchange and rated coefficient of performance $COP_{heat} = 4.5$, $COP_{cool} = 3.5$	Ductless air source heat pump. Rated coefficient of performance $COP = 5.0$
HVAC performance curves	Default Open Studio 3.5.1 software development kit performance curves used [62]	
HVAC set-points	heating: 20 °C, cooling 25.6 °C	
HVAC controls	Default control scheme used by EnergyPlus	
Smart ventilation	Yes	No
Waste heat exchange		
Gray water heat exchanger	Yes	No
Type	Horizontal (low efficiency)	
Coefficient (W/K/fixture)	3.00 (estimated for [63] with 1.5 m length and 62.5% efficiency)	
Ground heat exchange	Yes	No
Characteristics	Basalt with low thermal conductivity (0.693 W/m/K) and typical thermal capacity (2.35 MPa/K) [64]. Ten 76.2 m bore-holes (sensitivity shows 5 is sufficient but added capacity saves 0.15 kWh/m°C/yr). Ground temperature assumed to be 12 °C based on energy plus weather file input (Section 3.4). Default Open Studio piping and G-function settings were used. A target temperature of 23 °C is used to intermittently activate a constant speed pump for the ground heat exchange loop.	

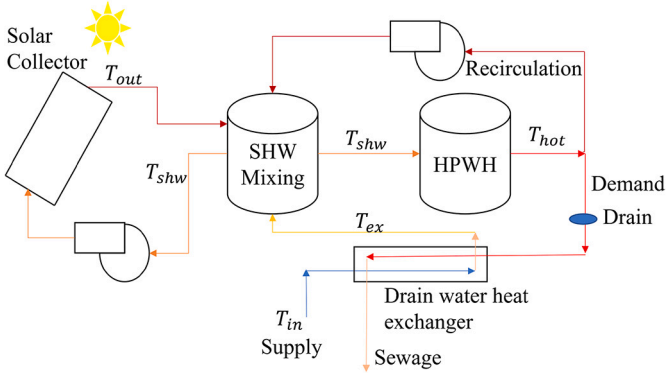

Fig. 4. Solar hot water system flow diagram for the PH.

rate inputs provide close to 0.6 air changes per hour of filtered air for the volume of each zone.

3.3.3. Solar hot water

A solar hot water system was added using snippets of code from the National Renewable Energy Laboratory water heater measure [72]. The system diagram in the PH is shown in Fig. 4 The system recycles waste heat through a drain water heat exchanger. Pre-heated water then enters a solar hot water mixing tank. The control pumps water out of this tank if the output temperature T_{out} from the solar collector is greater than the solar hot water mixing tank temperature T_{shw}. Otherwise, the pump is deactivated. This keeps the collector from becoming a heat rejector that wastes energy at night or during cloudy periods where heating is not possible. The pump also is deactivated if $T_{shw} > 48.8$ °C. This avoids sending water that is hotter than the setpoint T_{hot}.

3.4. Multiscenario extreme weather simulator

MEWS is a light-weight stochastic temperature history generator that increases mean dry bulb temperature according to an SSP scenario and also increases the frequency and intensity of HW events. Fig. 5 shows the steps to generate future scenario extreme heat and cold weather files and to apply these to Energy Plus models. MEWS was inspired by the need to understand HW impacts to buildings [73]. The first version published was only capable of working in Albuquerque, New Mexico to 2060 [74] while later versions can apply at any global position for which climate normals and daily summaries with maximum and minimum daily temperatures for 50 years or more are available.

The steps of the algorithm are listed below in the order shown in Fig. 5:

1. Using the NOAA daily summaries [75] and climate normals [76] for the nearest weather station available, calculate histograms for HW and CS. Fifty years of records are desirable to obtain sufficient amounts of data.
2. Use the methods from the original version of MEWS ([74]) to provide a good initial guess for 14 parameters for each month of the year.
3. Perform a genetic algorithm optimization to obtain good fits for each month using least squares squared sum error of duration and intensity histograms versus the output of the MEWS 14 parameter stochastic model. The stochastic model requires several hundred years of simulation to produce comparable histograms.
4. Calculate the Kolmogorov Smirnov test statistic to verify whether the optimization produced a good fit [77]. Many cases do not meet this criteria and have to be inspected manually. Often the failure is due to non-smooth histograms that can be overlooked because they have little bearing on worst case peak temperatures. The Kolmogorov-Smirnov test therefore cuts down the number of cases that need to be inspected manually and is not a final acceptance criterion. Regardless, the acceptance criterion is subjective and, in the results section, we show the worst case fits and resulting peak temperature distributions so that the study characteristics for future conditions are transparent.
5. Future frequency and intensity of extreme temperature events are driven by surface temperature change at the latitude and longitude of the location being analyzed. We use the average increase for a given SSP. MEWS can accept any combination of models from the Sixth Coupled Model Intercomparison Project (CMIP6). We use the same ensemble as for [28]. A polynomial fit over this ensemble is used to evaluate temperature anomaly from 1850-1900 for present and future times.
6. The future temperature anomaly is then used to shift intensity of HWs to match 10- and 50-year future thresholds per Figure SPM.6 of the IPCC 2021 summary for policy makers [29].
7. Once shifted, the MEWS model can be used to quickly generate thousands of scenarios where HW and CS events are generated randomly with a sinusoidal form.
8. The software then interposes the extreme temperature event scenarios onto hourly EnergyPlus weather files. These files must represent typical or climate normal conditions so that extreme temperature events are not included twice. The average temperature is increased by the future year's prediction for temperature anomaly from the polynmials calculated in step 5. The extreme temperature events are then added referenced to the climate normal daily average so that HW amplification is not counted twice since average conditions have already been shifted.
9. New EnergyPlus weather file files are then output with hundreds of files typically needed for each scenario to produce a good Monte-Carlo study.
10. The EnergyPlus weather file can then be run over any number of EnergyPlus models to produce a stochastic future scenario evaluation for building energy and thermal resilience assessments.

Our previous work provides mathematical formulation and detailed derivation of this process and the source code is open source software [28,78,79].

In this work, we analyzed NOAA data for the Santa Fe County Municipal Airport station ID USW00023049. We used the NOAA climate normals for 1991-2020 and daily summaries from 1941-2023. The daily summaries required gap filling from 1959-1996 using a Seasonal Auto Regressive Integrated Moving Average (SARIMA) model similar to our previous study [78]. We generated 200 files for 4 separate typical meteorological year (TMY) energy plus weather files for Santa Fe obtained from [55]: 1) TMY version 3 2) TMYx 2004-2018, 3) TMYx 2007-2021, and 4) U.S. climate normals 2006-2020. Files were generated for:

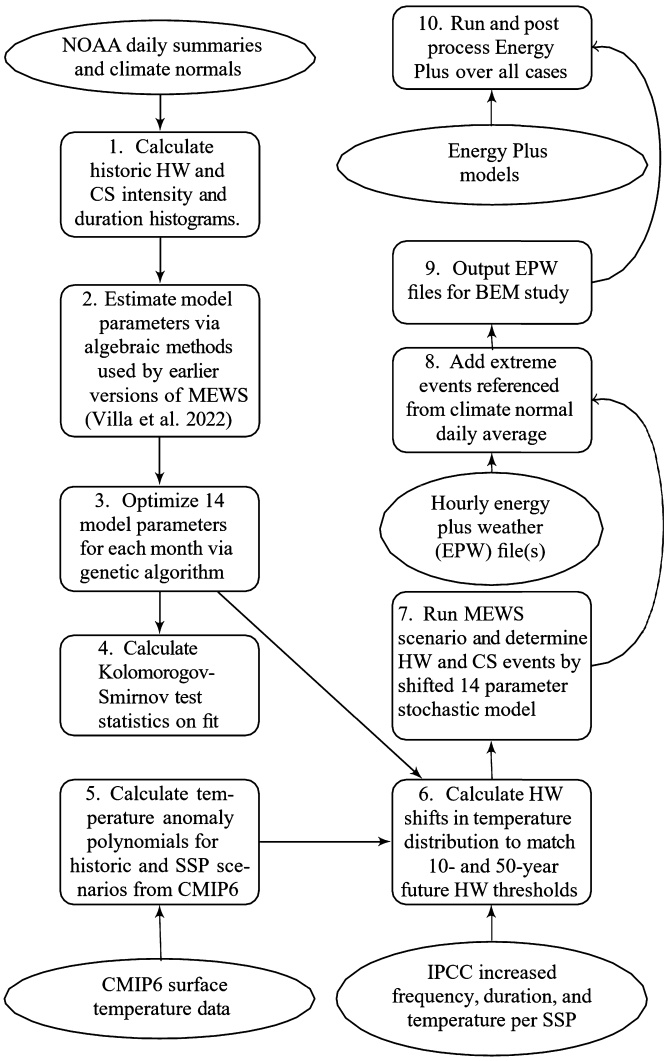

Fig. 5. MEWS algorithm flow diagram adapted from [78].

- 5%, 50%, and 95% IPCC confidence interval (CI) thresholds as specified in [28]
- 2020, 2040, 2060, and 2080
- SSP 2-4.5, 3-7.0, and 5-8.5 [30]

This led to a total of $4 \cdot 50 \cdot 3 \cdot 4 \cdot 3 = 7200$ weather files that were run for all eight EnergyPlus model configurations. This totals to 57,600 EnergyPlus runs for the MEWS dataset generated for this study.

3.5. Metrics

For energy metrics, we calculate the EUI which is the total yearly energy consumed for a specific category of energy use divided by the floor area of a building. We also use the maximum electric peak load for a year of EnergyPlus simulation.

For hot temperatures, we use the percent hours out of the year within the standard thermal resilience temperature ranges calculated in EnergyPlus where: 1) safe (S) = ($\leq 26.7\,^{\circ}C$) 2) caution (C) = ($> 26.7\,^{\circ}C, \leq 32.2\,^{\circ}C$), 3) extreme caution (EC) = ($> 32.2\,^{\circ}C, \leq 39.4\,^{\circ}C$), 4) danger (D) = ($> 39.4\,^{\circ}C, \leq 51.7\,^{\circ}C$), and extreme danger (ED) = ($> 51.7\,^{\circ}C$). The dryness of Santa Fe's climate makes neglecting humidity acceptable.

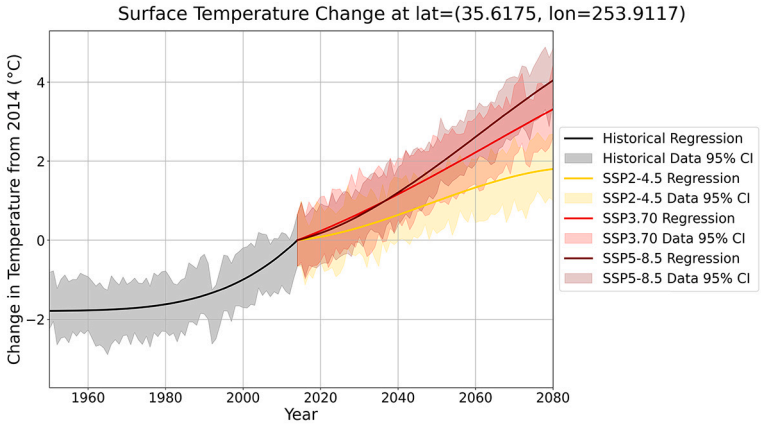

Fig. 6. Polynomials for CMIP6 ensemble. The gray and black show historic distribution and polynomial fit while yellow red and maroon show the three SSPs ensemble distributions and polynomial fits.

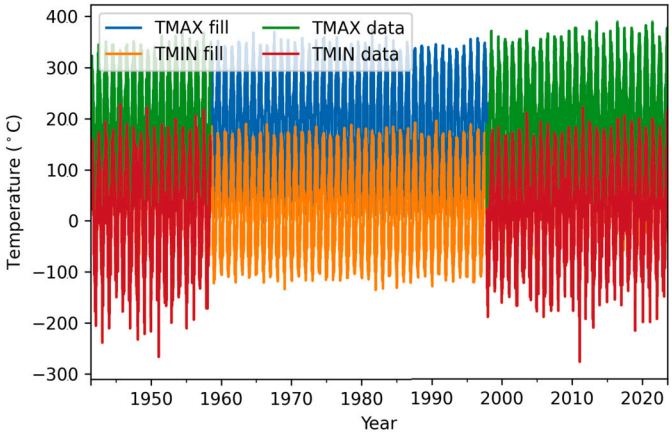

Fig. 7. SARIMA model gap filling for Santa Fe airport's NOAA daily summary data. Orange and blue show min and max temperatures for the gap filling model whereas green and red show the same for existing data.

For cold indoor temperatures, we use the percent hours out of the year in the following ranges: 1) cold caution (CC) = ($\leq 15.0°C, > 10.0°C$), cold extreme caution (CEC) = ($\leq 10.0°C, > 5.0°C$), cold danger (CD) = ($\leq 5.0°C, > 0.0°C$), cold extreme danger (CED) = ($\leq 0.0°C$).

4. Results

The future weather files generated by MEWS depend on an accurate fit to historic conditions. The results for the MEWS fit is therefore given first followed by energy consumption and then thermal resilience.

4.1. MEWS

The IPCC ensemble surface temperature rise for the three SSPs are shown in Fig. 6. MEWS uses the average values of the polynomial fits shown as solid lines near the center of the 95% CIs for the CMIP6 ensemble (see Table 1 of [28]).

The gap filling SARIMA model results are shown in Fig. 7. The large gap between 1959 and 1996 is shown in blue and orange whereas the existing data are shown in green and red. The MEWS fit to all of the data (gap filled and actual) in Fig. 7 for HWs was statistically significant using the 2-sided Kolmogorov-Smirnov p-value test for all months except February. Cold snaps did not have as good of fits with 6 months not passing the test. As a result, the fits were inspected manually for all months and no errors were found that were sufficient to warrant attention. Mostly, the MEWS model tended to miss sharp peaks leading to the poor p-value. Fig. 8 shows the worst case fit in February demonstrating that the failed test for both HWs and CSs is acceptable. For extreme temperature event durations, HWs failed for 6 months while CSs passed all months. The poor fits were all due to under-prediction of single day extreme event temperatures followed by over-prediction of 2-day heat waves. Longer heat waves, which are more consequential were accurately modeled as seen in Fig. 9. The model also exhibited the possibility of HWs that have duration nearly twice that of historic ones. Fig. 10 shows histograms of summary statistics for all 57,600 weather files generated by MEWS as verification that none of the files exhibited HW or CS that are unrealistic for Santa Fe's present and future climate to 2080. The worst case peak temperature is 58.9 °C occurring for the worst case conditions of 95% CI threshold for HW, SSP5-8.5 and 2080.

4.2. Energy consumption

Table 2 shows how energy consumption varies when current available ECWs are used instead of the high performance ones used by this study. The single run performed used the TMYx 2007-2021 [55] weather file for Santa Fe Municipal Airport.

Fig. 11 shows the energy performance with and without ECWs for both houses. Depicted are 2.5% and 97.5% probability thresholds at the bottom and top of the bars with maximum and minimum values displayed as an "x." The lines cross through the 50% probability threshold. As seen in the first row of the two left hand columns, total EUI increases for the PH while total EUI decreases in the right hand columns for the IECC dwelling. The second row shows that nearly the entire change is due to HVAC energy use. Adjacent columns for PH and IECC show that the ECWs decrease energy use for both cases. The fifth row shows that ECWs have little affect on peak loads with a slight decrease for the IECC dwelling. Table 3 shows the percent energy savings due to ECWs for the PH and IECC dwelling. Savings for the PH range from 1.32% to 3.12% for total EUI while the IECC dwelling ranges from 4.42% to 5.11% for total EUI.

The switching power per year for the 4 cases that include ECWs is shown in Fig. 12. The results are provided in kWh/day with less power needed by the PH than the IECC dwelling. The results shown are only for active switching with an assumed 3 min switch time (1 min was achieved in the lab). One can add 0.072 kWh/day to include the U.S. Department of Energy's maximum state maintenance.

4.3. Thermal resilience

The thermal resilience results for both models were filtered such that the most thermally resilient space was always counted. This is equivalent to the assumption that in extreme temperature conditions occupants can move to the safest thermal zone.

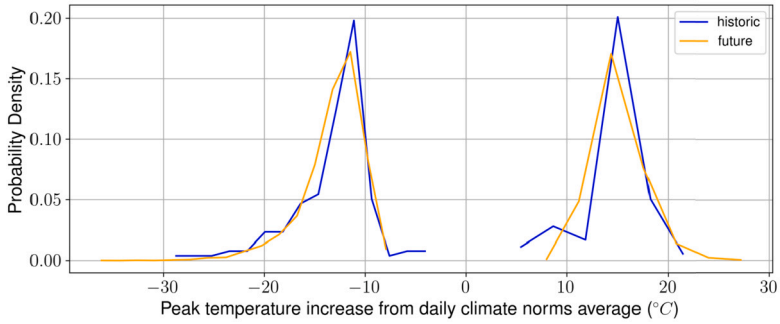

Fig. 8. MEWS worst case fit for February.

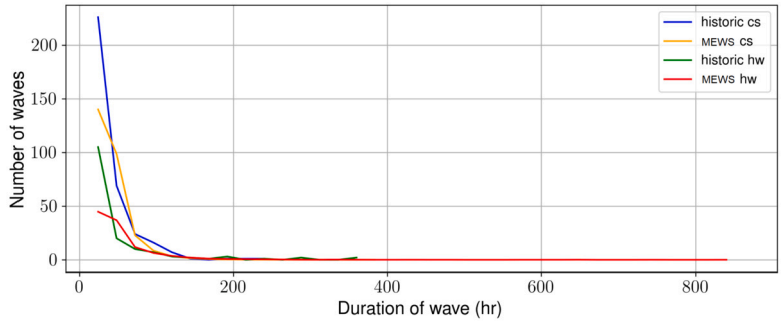

Fig. 9. MEWS worst case fit for duration in August.

Table 2
Comparing this study's high performance ECW to a typical ECW that is currently on the market for EE and thermal resilience (see section 3.1 for the properties).

		EUI (kWh/m^2)	Thermal Resilience			
			CC (hr)	C (hr)	CEC (hr)	EC (hr)
IECC dwelling	BL	97.14	1373	1043	66	1
	On the market ECW	93.51	1132	29	50	0
	Study ECW	92.84	838	34	32	0
PH	Baseline	47.66	18	224	0	0
	On the market ECW	46.91	0	35	0	0
	Study ECW	46.96	0	48	0	0

The ECWs have a positive effect on thermal resilience to both extreme hot and extreme cold for all cases with and without electricity. For extreme heat, Fig. 13 illustrates changes to percent hours in the year in the EC, D, and ED zones. Neither model exhibited time in ED with and without ECWs and electricity. The most notable change is for the IECC dwelling where the EC temperature range becomes a significant problem during the summer with as much as 8% of total yearly hours in this zone. This is reduced by a factor of 8 by incorporating ECW windows. Table 4 shows the change in hours in the C, EC, and D temperature ranges for the maxima and 95% probability interval calculated from the MEWS Monte-Carlo study.

For cold conditions, Fig. 14 shows the CC and CEC conditions in both models. Unlike hot conditions, extreme cold conditions are improved in this study by climate change. Table 5 shows the change in thermal resilience due to ECW. The PH is unaffected except that small improvements are present for some extreme cases for the 97.5% threshold and maximum case. Conversely, the IECC case has marked improvement for both CC and CEC conditions. Significant numbers of cases with CD and CED conditions were not present.

5. Discussion

The results of this study provide a rich comparative basis for answering our two research questions.

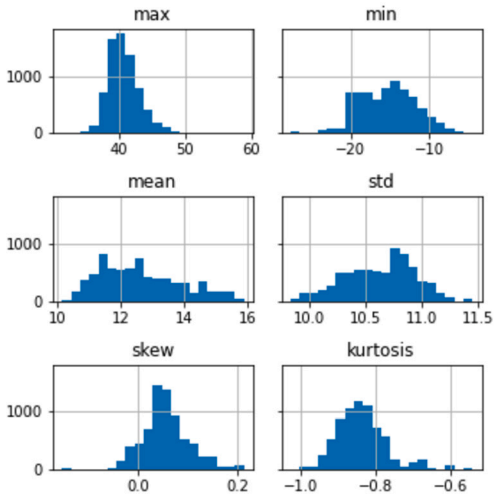

Fig. 10. MEWS summary statistics for 56,700 files. The horizontal axis is Dry bulb temperature (°C) or change in °C.

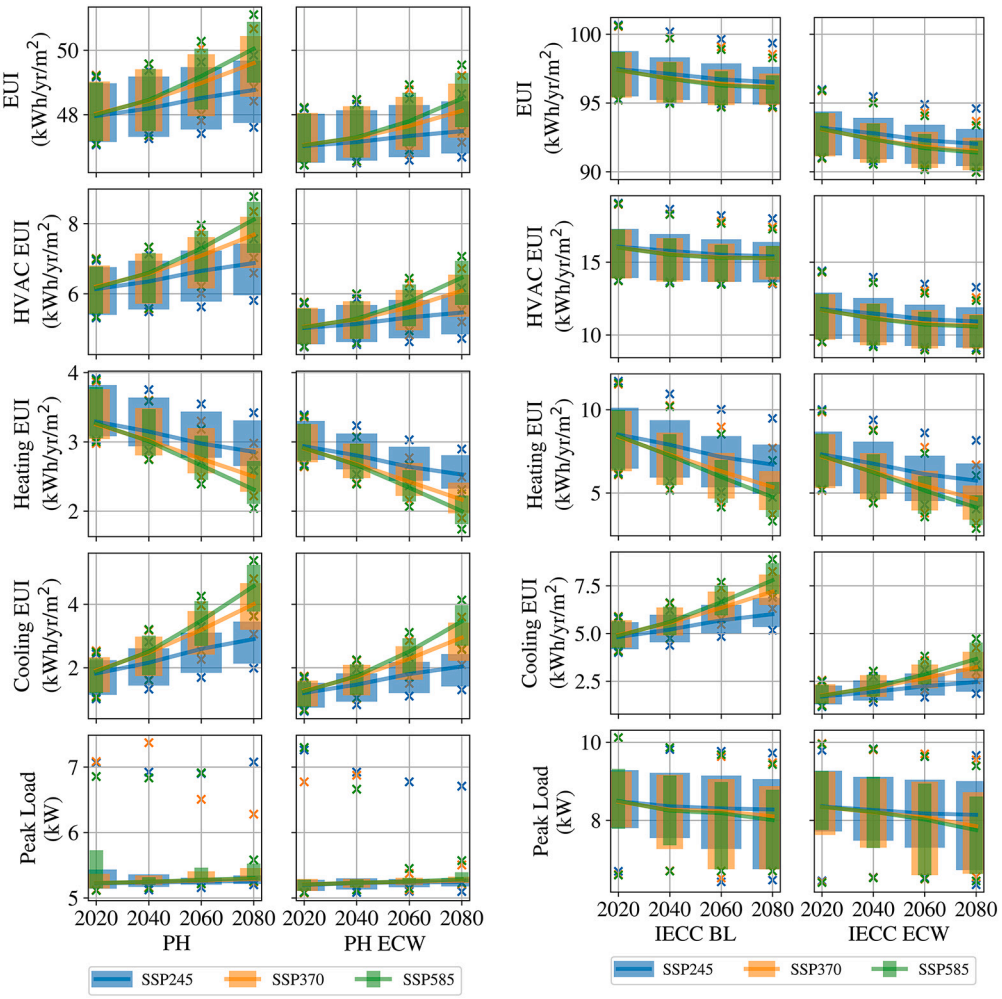

Fig. 11. PH and IECC dwelling EUI and peak load results. Solid lines show the mean while the ends of bars show the 2.5% and 97.5% probability thresholds. The "x" marks show sample minimum and maximum values. Looking at the two left hand or two right hand columns allows comparison of how ECWs reduce energy consumption for total, heating, and cooling EUIs.

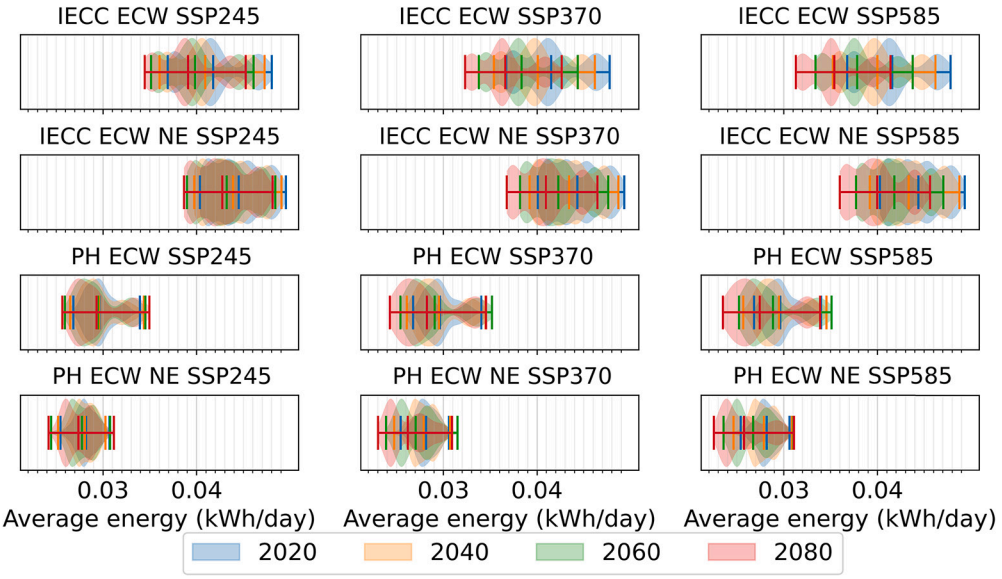

Fig. 12. Switching power per day for ECW cases with and without electricity.

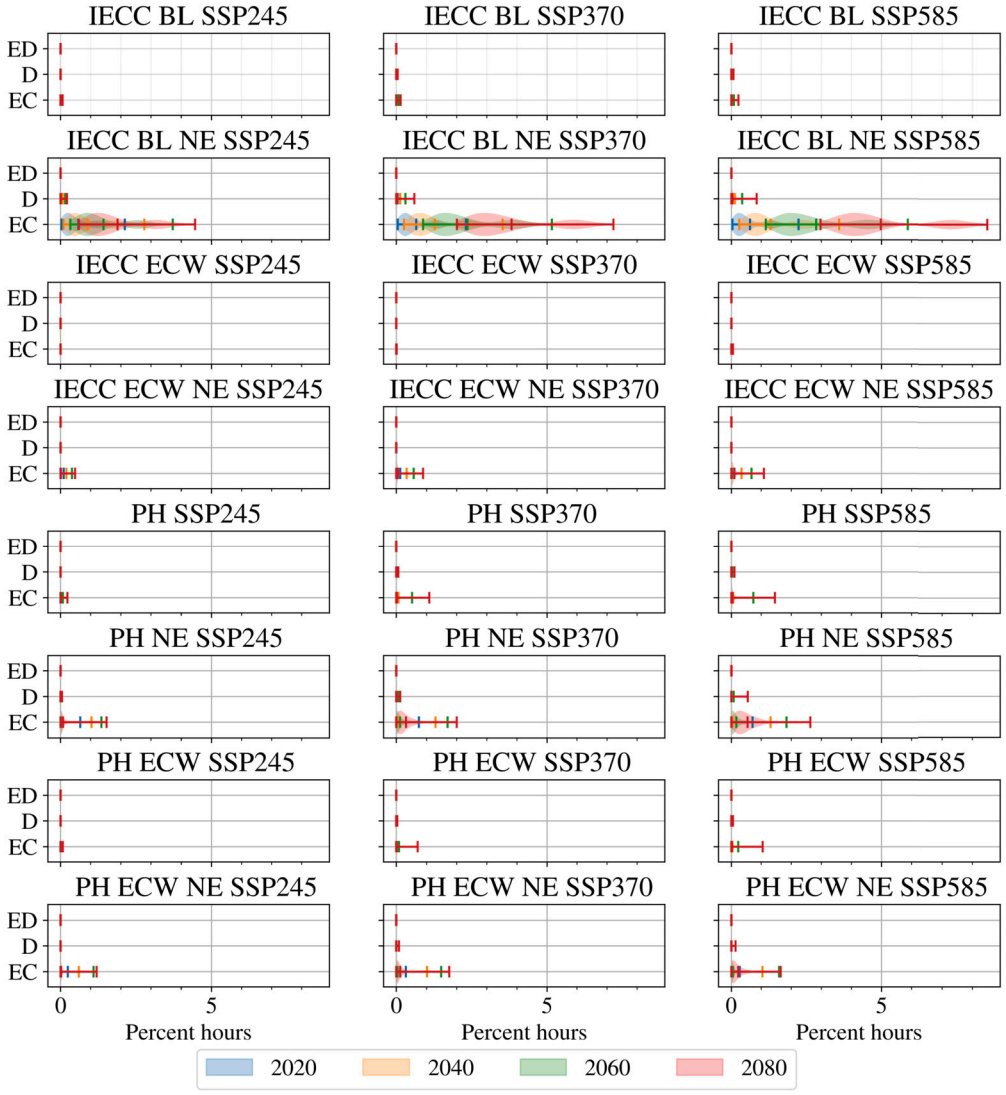

Fig. 13. Thermal resilience by IECC dwelling (IECC BL, IECC BL NE, IECC ECW, and IECC ECW NE) and the PH (PH, PH NE, PH ECW, and PH ECW NE).

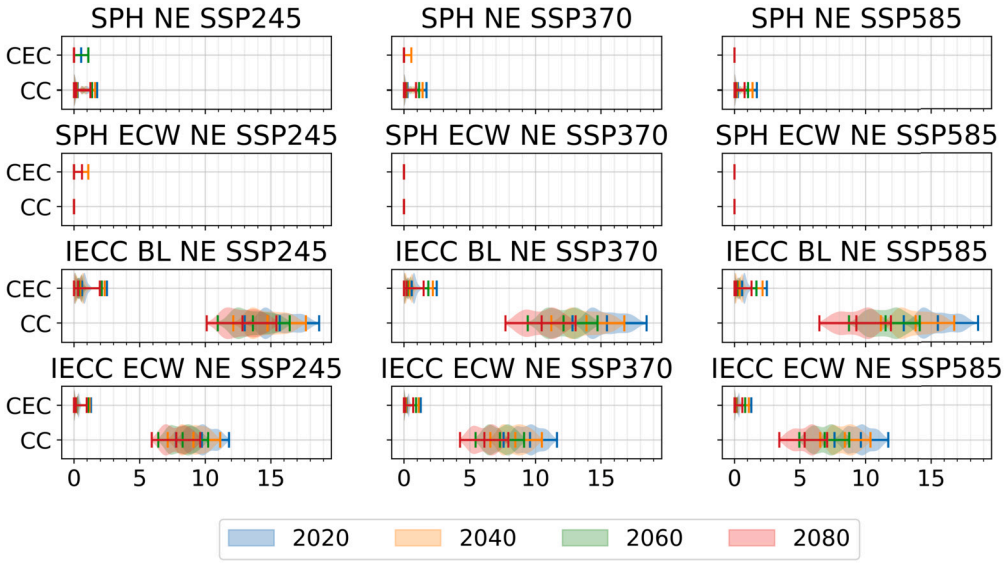

Fig. 14. Percent hours in the CC ($\leq 15.0\,°C, > 10.0\,°C$) and CEC ($\leq 10.0\,°C, > 5.0\,°C$).

Table 3
Percentage change in energy metrics due to ECWs for the PH and IECC dwelling.

			min	p025	p50	p975	max
PH EUI	SSP245	2020	1.327121	1.364343	1.939595	1.940035	1.973240
		2040	1.588864	1.560196	2.164622	2.126337	2.126228
		2060	1.737668	1.802935	2.430841	2.377115	2.289157
		2080	1.939986	1.993112	2.616160	2.545473	2.399360
	SSP370	2020	1.382423	1.382042	2.013005	1.992106	2.038062
		2040	1.683974	1.720241	2.386831	2.329147	2.251709
		2060	2.153974	2.174516	2.726533	2.649547	2.574652
		2080	2.634829	2.614330	2.987274	2.923780	2.871755
	SSP585	2020	1.382619	1.392630	1.979513	1.967391	1.998650
		2040	1.683502	1.751686	2.399561	2.339024	2.238006
		2060	2.338453	2.363443	2.836305	2.734634	2.682701
		2080	2.828777	2.822455	3.093468	3.120919	3.055122
PH HVAC EUI	SSP245	2020	15.625000	15.498155	18.029237	17.632898	17.669532
		2040	16.949153	16.650718	19.037657	18.170510	17.877095
		2060	17.591499	18.003565	19.920120	19.441064	18.361836
		2080	18.628571	18.624554	20.531401	19.729669	18.437226
	SSP370	2020	16.004963	15.969466	18.371719	17.725997	17.725118
		2040	17.303103	17.490119	19.797980	19.036996	18.313690
		2060	19.558011	19.351354	20.805998	19.775305	18.835616
		2080	21.068548	20.620438	20.761246	20.113544	19.426752
	SSP585	2020	15.776398	15.899005	18.191604	17.707568	17.758784
		2040	17.380952	17.687942	19.838872	19.169640	18.206522
		2060	20.320856	19.928788	20.856102	19.597647	19.031720
		2080	21.172023	20.701641	20.393120	19.448084	19.393939
IECC EUI	SSP245	2020	4.423610	4.496843	4.375887	4.439817	4.660752
		2040	4.537037	4.518494	4.449194	4.477354	4.684164
		2060	4.677355	4.647775	4.578564	4.562074	4.747475
		2080	4.709472	4.711103	4.640250	4.621391	4.786022
	SSP370	2020	4.452372	4.484673	4.430952	4.482036	4.665999
		2040	4.649007	4.606221	4.549591	4.556540	4.728878
		2060	4.753054	4.814324	4.731758	4.660147	4.824172
		2080	4.904306	5.001873	4.815493	4.804131	4.952770
	SSP585	2020	4.438573	4.479083	4.404547	4.487596	4.663666
		2040	4.649622	4.620069	4.550774	4.560133	4.730667
		2060	4.782782	4.881284	4.743238	4.692024	4.872154
		2080	4.994687	5.114269	4.914600	4.882595	5.004480
IECC HVAC EUI	SSP245	2020	30.558097	30.043161	26.703211	25.306204	24.422442
		2040	31.583794	30.946011	27.272727	25.913541	25.033738
		2060	32.342007	32.258065	28.548256	27.136975	25.846579
		2080	32.618826	32.902033	28.962418	27.378805	26.275332
	SSP370	2020	30.733945	30.294651	26.886792	25.764599	24.602122
		2040	32.252085	31.912835	28.317152	26.947193	25.635739
		2060	32.959851	33.489391	29.655455	28.050618	26.836158
		2080	33.921933	34.288058	30.255565	28.972711	27.870036
	SSP585	2020	30.614115	30.223864	26.729560	25.654155	24.553276
		2040	32.189239	32.100329	28.304947	27.004539	25.671025
		2060	33.426704	33.736742	29.946524	28.380294	27.136752
		2080	34.466912	34.622302	30.781893	29.539824	28.404953

5.1. Energy efficiency

A clear outcome seen in Table 2 is that the high performance ECW does not add value in comparison to current on the market ECW for the PH whereas the IECC dwelling performance is improved. The slight increase from the high performance ECW could probably be overcome with more tint states such that the wider band changes in SHGC and VT are only applied when advantageous. We therefore think that better controls may provide the high performance ECW with equal or slightly better performance than the on the market ECW. Regardless, not much EE improvement due to higher performance ECW is expected over current on the market ECW.

For the climate study, observation of Figs. 11 provides quantitative answers to how ECWs affect EE in the two high efficiency homes. Table 3 shows that ECWs have significant positive effects on EE in both present and future conditions for both houses. The statistical variation across 600 runs for each SSP, model configuration, and future year provide a 95% CI that estimates bounds for this positive effect in the future. It is also clear that less benefit is derived for all metrics for the PH than the IECC dwelling. From this, we see that ECWs have the least effect on the most efficient types of buildings. For both houses, climate change leads to greater energy savings for future conditions due to ECWs. This is primarily due for our case in Santa Fe to the ECW being effective at reducing future cooling loads. Opposite to total savings, the growth in energy savings in the future for the PH is greater than for the IECC dwelling.

Because of its high efficiency and C_w value of 0.51, the PH has energy savings on the low end of other studies in the literature that analyze BEM and ECW [51,53,80]. On the other hand, the IECC dwelling compares well to other studies. The results in the second row of Fig. 11 show 16% and 26% energy savings for HVAC which is comparable to literature values for HVAC in residential buildings. For example, Lee and Song experimentally measured cooling energy savings of 16.2-20.5% for cases with and without a tinted state [81]. Also, a study with attributes very similar to the IECC dwelling is given by Fekri et al. whose New Mexico single story residential case with and without an active window exhibited 16.7-26.3% energy savings for HVAC for several scenarios of control and smart window type [52]. We estimate a C_w value of 0.22 for Fekri et al. making it nearly equivalent to the IECC dwelling. This shows that the savings magnitude calculated here are reasonable. HVAC loads

Table 4
Change in percent hours within D, EC, and C temperature ranges due to ECWs during permanent power outage conditions. The columns contain probability thresholds 2.5%, 50.0%, and 97.5% and the minimum and maximum values for each sample of 600 runs. No change was exhibited for D values below the 97.5% threshold.

			D		EC					C				
			97.5%	max	min	2.5%	50.0%	97.5%	max	min	2.5%	50.0%	97.5%	max
IECC	SSP245	2020	0.00	0.00	0.00	0.00	0.00	0.00	0.00	0.00	0.00	−0.16	−0.66	−0.89
		2040	0.00	0.00	0.00	0.00	0.00	0.00	−0.04	0.00	−0.02	−0.25	−0.91	−1.24
		2060	0.00	0.00	0.00	0.00	0.00	0.00	−0.05	−0.01	−0.06	−0.35	−1.17	−1.58
		2080	0.00	0.00	0.00	0.00	0.00	0.00	−0.06	−0.02	−0.07	−0.43	−1.44	−1.83
	SSP370	2020	0.00	0.00	0.00	0.00	0.00	0.00	−0.02	0.00	0.00	−0.18	−0.73	−0.96
		2040	0.00	0.00	0.00	0.00	0.00	0.00	−0.05	0.00	−0.05	−0.32	−1.11	−1.49
		2060	0.00	0.00	0.00	0.00	0.00	−0.00	−0.08	−0.03	−0.09	−0.52	−1.63	−2.11
		2080	0.00	−0.05	0.00	0.00	0.00	−0.07	−0.14	−0.11	−0.21	−0.81	−2.49	−2.99
	SSP585	2020	0.00	0.00	0.00	0.00	0.00	0.00	−0.01	0.00	0.00	−0.17	−0.71	−0.95
		2040	0.00	0.00	0.00	0.00	0.00	0.00	−0.05	0.00	−0.06	−0.34	−1.13	−1.51
		2060	0.00	−0.03	0.00	0.00	0.00	−0.02	−0.09	−0.06	−0.13	−0.62	−1.91	−2.38
		2080	0.00	−0.08	0.00	0.00	0.00	−0.11	−0.18	−0.27	−0.40	−1.13	−3.03	−3.48
IECC NE	SSP245	2020	0.00	−0.03	−0.02	−0.04	−0.38	−1.71	−2.03	−9.64	−9.96	−11.34	−10.01	−9.66
		2040	0.00	−0.07	−0.10	−0.18	−0.65	−2.32	−2.59	−10.76	−10.91	−11.48	−9.66	−9.58
		2060	−0.04	−0.15	−0.32	−0.44	−1.13	−3.14	−3.35	−11.70	−11.69	−11.40	−9.19	−9.18
		2080	−0.06	−0.21	−0.61	−0.77	−1.56	−3.79	−3.98	−11.65	−11.72	−11.21	−8.81	−8.65
	SSP370	2020	0.00	−0.04	−0.04	−0.08	−0.44	−1.90	−2.17	−9.92	−10.18	−11.43	−9.93	−9.64
		2040	−0.03	−0.13	−0.25	−0.36	−1.00	−2.91	−3.19	−11.47	−11.50	−11.43	−9.35	−9.23
		2060	−0.10	−0.30	−0.89	−1.09	−1.97	−4.41	−4.59	−11.46	−11.57	−10.87	−8.43	−8.33
		2080	−0.20	−0.60	−2.01	−2.13	−3.35	−6.24	−6.32	−10.80	−10.96	−9.80	−7.08	−7.15
	SSP585	2020	0.00	−0.04	−0.04	−0.06	−0.41	−1.82	−2.12	−9.82	−10.08	−11.38	−9.94	−9.61
		2040	−0.04	−0.13	−0.27	−0.38	−1.03	−2.96	−3.24	−11.55	−11.56	−11.42	−9.33	−9.23
		2060	−0.12	−0.37	−1.16	−1.44	−2.40	−5.10	−5.20	−11.09	−11.34	−10.54	−8.00	−7.95
		2080	−0.40	−0.85	−2.97	−3.21	−4.38	−7.43	−7.40	−10.32	−10.47	−8.98	−6.12	−6.15
PH	SSP245	2020	0.00	0.00	0.00	0.00	0.00	0.00	−0.00	0.00	0.00	−0.14	−0.43	−0.53
		2040	0.00	0.00	0.00	0.00	0.00	0.00	−0.03	0.00	−0.01	−0.21	−0.64	−0.62
		2060	0.00	0.00	0.00	0.00	0.00	0.00	−0.02	0.00	−0.07	−0.35	−0.67	−0.95
		2080	0.00	0.00	0.00	0.00	0.00	0.00	−0.15	−0.04	−0.10	−0.43	−0.77	−1.18
	SSP370	2020	0.00	0.00	0.00	0.00	0.00	0.00	−0.02	0.00	0.00	−0.14	−0.43	−0.58
		2040	0.00	0.00	0.00	0.00	0.00	0.00	−0.03	0.00	−0.05	−0.29	−0.72	−0.81
		2060	0.00	0.00	0.00	0.00	0.00	−0.03	−0.44	−0.08	−0.12	−0.51	−1.22	−1.19
		2080	0.00	−0.03	0.00	0.00	0.00	−0.07	−0.38	−0.68	−0.86	−1.45	−2.34	−2.80
	SSP585	2020	0.00	0.00	0.00	0.00	0.00	0.00	−0.02	0.00	0.00	−0.14	−0.46	−0.56
		2040	0.00	0.00	0.00	0.00	0.00	0.00	−0.03	0.00	−0.06	−0.30	−0.73	−0.83
		2060	0.00	−0.03	0.00	0.00	0.00	−0.02	−0.51	−0.20	−0.23	−0.66	−1.69	−1.42
		2080	−0.01	−0.05	0.00	0.00	0.00	−0.16	−0.41	−1.51	−1.52	−2.81	−3.24	−4.19
PH NE	SSP245	2020	0.00	0.00	0.00	0.00	0.00	−0.03	−0.41	−0.28	−0.33	−1.30	−2.02	−2.09
		2040	0.00	0.00	0.00	0.00	0.00	−0.11	−0.42	−0.80	−0.85	−2.33	−2.76	−2.80
		2060	0.00	0.00	0.00	0.00	0.00	−0.22	−0.27	−1.34	−1.71	−3.77	−3.54	−3.67
		2080	0.00	−0.05	0.00	0.00	−0.02	−0.37	−0.33	−1.96	−2.40	−4.43	−3.81	−4.04
	SSP370	2020	0.00	0.00	0.00	0.00	0.00	−0.06	−0.43	−0.46	−0.48	−1.57	−2.20	−2.25
		2040	0.00	0.00	0.00	0.00	0.00	−0.20	−0.28	−1.11	−1.54	−3.41	−3.29	−3.59
		2060	0.00	−0.07	0.00	0.00	−0.06	−0.40	−0.21	−2.83	−3.03	−4.43	−4.14	−4.05
		2080	−0.03	−0.04	0.00	0.00	−0.16	−0.79	−0.25	−4.30	−5.17	−4.43	−4.76	−4.53
	SSP585	2020	0.00	0.00	0.00	0.00	0.00	−0.05	−0.43	−0.40	−0.42	−1.43	−2.11	−2.20
		2040	0.00	0.00	0.00	0.00	0.00	−0.22	−0.27	−1.15	−1.59	−3.54	−3.38	−3.65
		2060	0.00	−0.09	0.00	0.00	−0.10	−0.40	−0.25	−3.24	−3.76	−4.50	−4.31	−4.17
		2080	−0.04	−0.41	0.00	0.00	−0.31	−0.47	−0.98	−5.19	−5.47	−4.71	−4.72	−4.32

only comprise 12% and 17% of the PH and IECC dwelling total energy respectively making the total savings potential much smaller than cases with less efficient HVAC or envelope. For example, before the PH design was optimized, significant energy savings were exhibited because the WWR was too high. This was creating too much heat leading to excessive cooling in the summer that was then negated by the presence of ECW. Under such suboptimal PH design, total building energy savings due to the ECW was much higher.

The PH is predicted to become less efficient into the future due to its high C_w value of 0.51. On the other hand, the IECC dwelling's C_w value of 0.20 leads to reductions of 1.0-1.4% for heating in comparison to the 2020 results. For the PH, performance degrades by 1.5-4.0% for total building energy. This indicates that high-end insulation and hotter conditions will make solar passive design less important in the future. Windows will continue to be used but they will transition toward not contributing to efficiency in comparison to a structure with no windows that has improved insulation as a result.

5.2. Thermal resilience

On the market ECW perform just as well as our high performance ECW for the PH but perform a little less well for the IECC dwelling as seen in Table 2.

For the climate study, the PH is more thermally resilient than the IECC dwelling with the ECW making only small improvements to the PH performance. Much more marked improvements are present for the IECC dwelling. The results also show that the IECC dwelling begins to have significant thermal resilience issues in the absence of ECW during future extreme HWs conditions that currently do not exist. The results found up to 1% of hours (87.6 hours/yr) being in the danger (D) temperature range. Keeping low-power ECWs active nearly eliminates this danger zone with less than a day of time in D conditions. ECWs also reduce drastically the EC range by as much as a factor of 8. Though thermal resilience is improved slightly for the PH by reducing hours of exposure to EC by a maximum of 0.98% for the worst case future analyzed, PH designs remain safe regardless of the presence of ECW in

Table 5
Change in percent hours within CC and CEC temperature ranges due to ECWs during permanent power outage conditions. The columns contain probability thresholds 2.5%, 50.0%, and 97.5% and the minimum and maximum values for each sample of 600 runs. No change was exhibited for CD and CED values.

			CC					CEC				
			min	2.5%	50.0%	97.5%	max	min	2.5%	50.0%	97.5%	max
PH NE	SSP245	2020	0.00	0.00	−0.02	−1.13	−1.76	0.00	0.00	0.00	0.00	−0.55
		2040	0.00	0.00	0.00	−0.97	−1.61	0.00	0.00	0.00	0.00	0.00
		2060	0.00	0.00	0.00	−0.80	−1.37	0.00	0.00	0.00	0.00	−1.10
		2080	0.00	0.00	0.00	−0.69	−1.24	0.00	0.00	0.00	0.00	0.61
	SSP370	2020	0.00	0.00	−0.02	−1.07	−1.71	0.00	0.00	0.00	0.00	0.00
		2040	0.00	0.00	0.00	−0.85	−1.40	0.00	0.00	0.00	0.00	−0.55
		2060	0.00	0.00	0.00	−0.60	−1.15	0.00	0.00	0.00	0.00	0.00
		2080	0.00	0.00	0.00	−0.45	−0.91	0.00	0.00	0.00	0.00	0.00
	SSP585	2020	0.00	0.00	−0.02	−1.07	−1.71	0.00	0.00	0.00	0.00	0.00
		2040	0.00	0.00	0.00	−0.84	−1.39	0.00	0.00	0.00	0.00	0.00
		2060	0.00	0.00	0.00	−0.55	−1.04	0.00	0.00	0.00	0.00	0.00
		2080	0.00	0.00	0.00	−0.38	−0.79	0.00	0.00	0.00	0.00	0.00
IECC NE	SSP245	2020	−5.25	−5.45	−5.74	−6.50	−6.86	0.00	−0.01	−0.47	−0.72	−1.22
		2040	−5.01	−5.25	−5.53	−6.22	−6.52	0.00	0.00	−0.38	−0.62	−1.14
		2060	−4.55	−4.74	−5.15	−6.05	−6.22	0.00	0.00	−0.23	−0.47	−1.04
		2080	−4.20	−4.45	−4.96	−5.63	−5.81	0.00	0.00	−0.22	−0.46	−0.99
	SSP370	2020	−5.25	−5.53	−5.67	−6.42	−6.83	0.00	−0.01	−0.46	−0.70	−1.21
		2040	−4.65	−4.87	−5.23	−6.01	−6.29	0.00	0.00	−0.25	−0.48	−1.06
		2060	−3.97	−4.30	−4.74	−5.37	−5.61	0.00	0.00	−0.18	−0.42	−0.94
		2080	−3.46	−3.72	−4.32	−5.07	−5.13	0.00	0.00	−0.09	−0.39	−0.79
	SSP585	2020	−5.29	−5.54	−5.65	−6.44	−6.86	0.00	−0.01	−0.46	−0.68	−1.19
		2040	−4.62	−4.81	−5.21	−5.99	−6.39	0.00	0.00	−0.25	−0.47	−1.05
		2060	−3.78	−4.03	−4.58	−5.15	−5.37	0.00	0.00	−0.16	−0.38	−0.87
		2080	−3.05	−3.29	−3.98	−4.65	−4.85	0.00	0.00	−0.08	−0.25	−0.70

future extreme conditions. We therefore conclude that the PH's thermal mass, shading, and smart ventilation are sufficient to keep the PH thermally resilient without ECWs. This is not the case for the IECC dwelling. ECWs are therefore a greater asset to less efficient designs for thermal resilience.

5.3. PH and ECWs design

Many details of the PH design need further specification for actual implementation. Fig. 12 makes it clear that the switching power is likely to be low enough for a local battery solution depending on the state maintenance power required. We know that the EChr film will need little to no power when switching is not occurring but have not yet made the necessary measurements. A small solar charger on the window could also likely be used to create designs that operate independently. Such solutions may not be reliable for long stretches of cloudy weather. Under such circumstances, the window solar performance will not be very important though. Climate change helps reduce the power needed for active switching as seen in Fig. 12. The passive house exhibits lower switch power because the solar passive design provides a more stable temperature profile than the IECC dwelling which is a result of the greater thermal mass stabilizing temperature fluctuations. For the ECWs, more sophisticated controls that balance thermal and visual comfort are needed. The simple controls used in this study focus on energy performance so that present and future temperature conditions can be assessed. Adding active blinds with insulation could further reduce the need for HVAC and increase the visual comfort of the design.

The smart ventilation feature of the PH serves to assure high indoor air quality and economization. Though more energy intensive than natural ventilation, the need for protection against wildfire or dusty conditions during wind makes it highly desirable to accept the pressure drops included by MERV-13 filters. Increased protection is also afforded through in-room use of HEPA air filters with UV light sanitizing and ionizers. The controls for ventilation used in this study are the simplest possible. Additional efficiency may be able to be achieved if continued research investigated more sophisticated controls. The high EE already achieved before ECW installation here makes returns on such additional complexity minimal though. We have also neglected visual comfort and adjustment of lighting energy in this study. The lighting energy levels seen in Table 1 has already been given a level of energy consumption that can supply needs at all times. Such lighting controls would therefore reduce lighting loads in comparison to our models.

The EChr film that inspired our selection of ECW properties needs to be further evaluated under a range of temperatures. A comparable study by Nowacki and Walesa-Chorab indicates that similar materials have degraded performance at low temperature and increased performance at high temperatures [21]. The increased performance comes at the expense of EChr life time though.

Concerning potential reductions in cost for ECWs, the materials used to produce the results we analyzed do not require any strategic mineral feedstock. Also they could be deposited through a roll-to-roll process, unlike the current standard ECW materials. Further development is needed to analyze whether these potentials can produce actual cost savings for full scale window assemblies.

5.4. MEWS

The fits to MEWS were acceptable, but could use improvement. The biggest limitation was the lack of more than 50 years of data for the study. Regardless, the ranges of temperature exhibited in Fig. 10 explicitly shows the distributions generated. Though this study is the most thorough method yet applied to stochastic futures for high performance houses, there is much work yet to be done to assure that the future weather simulated spans the range of possibilities for future conditions from the CMIP6 model ensemble.

6. Conclusion

This study has established how EE and thermal resilience are enhanced by ECWs for high performance houses in Santa Fe given present and future conditions. The results have established that the IECC dwelling (i.e, IECC 2021 compliant) saves more energy (4.4-5.1%) using ECWs than the PH presented (1.3-3.1%). The PH is nearly twice as efficient though, demonstrating that extremely efficient systems cannot become much more efficient. For resilience, the ECW reduce hours in danger or cautionary temperature zones for both cases. The PH remains

safe to 2080 whereas the IECC dwelling without ECWs begins to exhibit cases where dangerous thermal conditions exist for significant amounts of time. ECWs overcome this issue.

The differences in performance between the PH and IECC dwelling indicate that studies like this one need to be carried out over a broad range of EE measures. This is urgent as governments seek policies to most effectively mitigate and adapt to climate change. New kinds of analyses that combine resilience and techno-economic assessments are needed to balance the complex set of competing priorities in climate actions. When evaluating window and building systems, it is important to consider EE, thermal comfort, cost-effectiveness, and environmental impact [17]. This study has focused on the first two of these as a function of future extreme temperature events. An important follow-on is to extend the stochastic analysis we have performed to include cost-effectiveness and environmental impact. Both of these are required to understand net-zero building performance in the future. Such work will provide economic measures with CIs of climate change scenarios.

In addition to the improvements ECWs provide for EE and thermal resilience, visual comfort may be markedly enhanced with occupancy sensors included in the control loop. Future work should consider how much visual comfort can be enhanced by the ECW with as little EE compromise as possible. Also, future work should consider buildings that represent a continuum of C_w values to see how EE, thermal resilience and ECWs interact. Optimization of the low-power ECW technology in modular construction is also of interest for future work [82]. A study of the likelihood of power outages in Santa Fe could also provide a way to use the thermal resilience results to understand the probability of thermally difficult or dangerous conditions rather than using the worst case scenario where power is always off for an entire year. There is also a need to obtain a better record of daily maximum and minimum temperatures in Santa Fe to enable obtaining better MEWS fits. Finally, the lack of previous studies that look at how the future will affect ECW performance for a given location makes it evident that a multi-climate study of future conditions across many building types is needed.

Disclaimer

Sandia National Laboratories is a multimission laboratory managed and operated by National Technology and Engineering Solutions of Sandia LLC, a wholly owned subsidiary of Honeywell International Inc. for the U.S. Department of Energy's National Nuclear Security Administration under contract DE-NA0003525. This paper describes objective technical results and analysis. Any subjective views or opinions that might be expressed in the paper do not necessarily represent the views of the U.S. Department of Energy or the United States Government.

Glossary

BEM	building energy model
BL	Baseline
C	caution
CC	cold caution
CD	cold danger
CEC	cold extreme caution
CED	cold extreme danger
CI	confidence interval
CMIP6	the Sixth Coupled Model Intercomparison Project
CS	cold snap
D	danger
EC	extreme caution
EChr	Electrochromic
ECW	electrochromic window
ED	extreme danger
EE	Energy efficiency
EMS	energy management system
EUI	energy use intensity
GHG	green house gas
HVAC	heating ventilation and air conditioning
HW	heat wave
IECC	International Energy Conservation Code
IPCC	Intergovernmental Panel on Climate Change
MERV	minimum efficiency reporting value
MEWS	multiscenario extreme weather simulator
NE	no electricity
NOAA	National Oceanic Atmospheric Administration
PH	passive house
SARIMA	Seasonal Auto Regressive Integrated Moving Average
SHGC	solar heat gain coefficient
SSP	shared socioeconomic pathway
TMY	typical meteorological year
TMYx	TMY version X
U.S.	United States
VT	visible transmittance
WWR	window to wall ratio

CRediT authorship contribution statement

Daniel L. Villa: Was the principal investigator and did all BEM modeling, MEWS analysis, data curation, and major writing for this paper except for section 3.1. **Nathan Hahn and John Grey** provided services as investigators. They provided all laboratory results for the polymeric ECW. Nathan provided review of the entire paper and writing of 3.1 and a paragraph in the introduction. **Frances Pavich:** Helped with funding acquisition via a New Mexico Small Business Assistance grant. She worked with the corresponding author to conceptualize the PH and provided information on the site such houses are planned to be built on.

CRediT authorship contribution statement

Daniel L. Villa: Writing – review & editing, Writing – original draft, Software, Methodology, Investigation, Formal analysis, Data curation, Conceptualization. **Nathan T. Hahn:** Writing – review & editing, Writing – original draft, Supervision, Resources, Project administration, Methodology, Investigation, Funding acquisition. **John K. Grey:** Validation, Investigation, Data curation. **Frances Pavich:** Resources, Funding acquisition, Conceptualization.

Declaration of competing interest

The authors declare the following financial interests/personal relationships which may be considered as potential competing interests:

Daniel L. Villa reports financial support was provided by United States Department of Energy Building Technology Office by grant NL0039169. Daniel L. Villa reports financial support was provided by Sandia National Laboratories Internal Research Funds. Daniel L. Villa reports financial support was provided by New Mexico Small Business Assistance. Nathan T Hahn reports was provided by Sandia National Laboratory Internal Research Funds. John K Grey reports financial support was provided by Sandia National Laboratory Internal Research Funds. Frances Pavich reports statistical analysis was provided by New Mexico Small Business Assistance. If there are other authors, they declare that they have no known competing financial interests or personal relationships that could have appeared to influence the work reported in this paper.

Data availability

The BEM created for this project are available on the MEWS Github site at [84]. The MEWS files have not been released. Please contact the corresponding author to inquire about obtaining them.

Acknowledgements

The authors would like to thank the New Mexico Small Business Association that provided a grant to perform 1/2 of this study. One quarter of the funding came from the Sandia National Laboratories Labs Directed Research and Development Program. The final quarter of the funding came from the U.S. Department of Energy Building Technologies Office Future Weather Project under contract number NL0039169 [83].

References

[1] Y. Ou, C. Roney, J. Alsalam, K. Calvin, J. Creason, J. Edmonds, A.A. Fawcett, P. Kyle, N. Kanishka, P. O'Rourke, P. Patel, S. Ragnauth, S.J. Smith, H. McJeon, Deep mitigation of co_2 and non-co_2 gases towards 1.5°c and 2°c futures, Nat. Commun. 12 (2021) 6245, https://doi.org/10.1038/s41467-021-26509-z.

[2] D. Reckien, A.K. Magnan, C. Singh, M. Lukas-Sithole, B. Orlove, E.L.F. Schipper, E.C. de Perez, Navigating the continuum between adaptation and maladaptation, Nat. Clim. Change 13 (2023) 907–918, https://doi.org/10.1038/s41558-023-01774-6.

[3] G.A. Meehl, C. Tebaldi, More intense, more frequent, and longer lasting heat waves in the 21st century, Science 305 (2004) 994–997, https://doi.org/10.1126/science.1098704.

[4] T. Cowan, A. Purich, S. Perkins, A. Pezza, G. Boschat, K. Sadler, More frequent, longer, and hotter heat waves for Australia in the twenty-first century, J. Climate 27 (15) (2014) 5851–5871, https://doi.org/10.1175/JCLI-D-14-00092.1.

[5] O. Mazdiyasni, M. Sadegh, F. Chiang, A. AghaKouchak, Heat wave intensity duration frequency curve: a multivariate approach for hazard and attribution analysis, Sci. Rep. 9 (2019), https://doi.org/10.1038/s41598-019-50643-w.

[6] C.W. Callahan, J.S. Mankin, Globally unequal effect of extreme heat on economic growth, Sci. Adv. 8 (43) (2022) eadd3726, https://doi.org/10.1126/sciadv.add3726, https://www.science.org/doi/pdf/10.1126/sciadv.add3726.

[7] Z. Ying-Xian, L. Yan-Ju, D. Yi-Hui, Identification of winter long-lasting regional extreme low-temperature events in Eurasia and their variation during 1948-2017, Adv. Clim. Change Res. 12 (3) (2021) 353–362, https://doi.org/10.1016/j.accre.2021.05.005.

[8] R.J. Hall, D.M. Mitchell, W.J.M. Seviour, C.J. Wright, Surface hazards in North-West Europe following sudden stratospheric warming events, Environ. Res. Lett. 18 (6) (2023), https://doi.org/10.1088/1748-9326/acd0c3.

[9] IEA, Global status report for buildings and construction 2019, Tech. Rep., International Energy Agency, 2019, https://www.iea.org/reports/global-status-report-for-buildings-and-construction-2019.

[10] U. N. E. Programme, 2022 global status report for buildings and construction: Towards a zero-emissions, efficient and resilient buildings and construction sector, Tech. Rep., United Nations, November 2022, www.globalabc.org, 2022.

[11] C. Harris, Pathway to zero energy windows, Tech. Rep., NREL, April 2022, https://www.nrel.gov/docs/fy22osti/80171.pdf.

[12] L.L. Fernandes, E.S. Lee, D. Dickerhoff, et al., Electrochromic Window Demonstration at the John E. Moss Federal Building, 650 Capital Mall Sacrameto, California, Lawrence Berkely National Laboratory Technical Report 2001183, 2023, https://doi.org/10.2172/1483274, https://escholarship.org/uc/item/8qk0m5vb.

[13] S. G. C. (SGC). Smart glass pricing [online], https://www.smartglasscountry.com/news/smart-glass-cost-and-smart-film-price. (Accessed 22 December 2023).

[14] R. Newcomb, How much do triple-pane windows cost? [online]. Blog by Rachel Newcomb, https://www.architecturaldigest.com/reviews/windows/triple-pane-windows-cost#:~:text=Larger%20windows%20require%20more%20glass,don%27t%20include%20installation%20costs, December 2023. (Accessed 22 December 2023).

[15] S.K. Pal, K. Alanne, J. Jokisalo, K. Siren, Energy performance and economic viability of advanced window technologies for a new Finnish townhouse concept, Appl. Energy 162 (2016) 11–20, https://doi.org/10.1016/j.apenergy.2015.10.056, https://www.sciencedirect.com/science/article/pii/S0306261915012830.

[16] Z. Zeng, J. Chen, G. Augenbroe, Movable window insulation as an instantiation of the adaptive building envelope: an investigation of its cost-effectiveness in the u.s, Energy Build. 247 (2021), https://doi.org/10.1016/j.enbuild.2021.111138.

[17] S.A. Moghaddam, C. Serra, M. Gameiro da Silva, N. Simões, Comprehensive review and analysis of glazing systems towards nearly zero-energy buildings: energy performance, thermal comfort, cost-effectiveness, and environmental impact perspectives, Energies 16 (17) (2023), https://doi.org/10.3390/en16176283, https://www.mdpi.com/1996-1073/16/17/6283.

[18] Wikipedia, Electrochromic device [online], https://en.wikipedia.org/wiki/Electrochromic_device, 2023. (Accessed 22 December 2023).

[19] S. Grewal, T.G. Habteyes, W.M. Takele, D. Chen, J.K. Grey, N.T. Hahn, Exceptional electrochromic solar modulation using polyanionic dopant templated poly (diphenylamine) thin films, ACS Appl. Opt. Mater. 2 (3) (2024) 361–367, https://doi.org/10.1021/acsaom.3c00421.

[20] R. Tällberg, B.P. Jelle, R. Loonen, T. Gao, M. Hamdy, Comparison of the energy saving potential of adaptive and controllable smart windows: a state-of-the-art review and simulation studies of thermochromic, photochromic and electrochromic technologies, Sol. Energy Mater. Sol. Cells 200 (2019) 109828, https://doi.org/10.1016/j.solmat.2019.02.041, https://www.sciencedirect.com/science/article/pii/S0927024819301072.

[21] M. Nowacki, M. Walesa-Chorab, Influence of temperature on electrochemical and electrochromic properties of naphthalenediimide-triphenylamine-based polymer, Prog. Org. Coat. 182 (2023) 107691, https://doi.org/10.1016/j.porgcoat.2023.107691, https://www.sciencedirect.com/science/article/pii/S0300944023002874.

[22] P.H. Institute, Criteria for buildings: Passive house – enerphit – phi low energy building version 10c valid with phpp 10, Tech. Rep., Passive House Institute, Jan 2023, https://passiv.de/downloads/03_building_criteria_en.pdf.

[23] PassiveHaus trust web-site [online], https://www.passivhaustrust.org.uk/. (Accessed 18 December 2023), 2023.

[24] IECC, 2021 international energy conservation code (iecc) [online], https://codes.iccsafe.org/content/IECC2021P1/index. (Accessed 29 August 2023), 2021.

[25] ASHRAE, Standard 169-2021 climatic data for building design standards, Tech. Rep., American Society for Heating, Refrigeration, and Air-Conditioning Engineers, 2021, https://www.techstreet.com/ashrae/standards/ashrae-169-2021?product_id=2238548.

[26] U.s. Climate resilience toolkit climate explorer [online], https://crt-climate-explorer.nemac.org. (Accessed 18 December 2023), 2023.

[27] NREL, Passive solar design strategies: Guidelines for home builders: Santa Fe, New Mexico, Tech. Rep., National Renewable Energy Laboratory (NREL), 1989, https://www.nrel.gov/docs/legosti/old/17273.pdf.

[28] D.L. Villa, T. Schostek, K. Govertsen, M. Macmillan, A stochastic model of future extreme temperature events for infrastructure analysis, Environ. Model. Softw. 163 (2023) 105663, https://doi.org/10.1016/j.envsoft.2023.105663, https://www.sciencedirect.com/science/article/pii/S136481522300049X.

[29] V. Masson-Delmotte, P. Zhai, A. Pirani, S.L. Connors, C. Péan, S. Berger, N. Caud, Y. Chen, L. Goldfarb, M.I. Gomis, M. Huang, K. Leitzell, E. Lonnoy, J. Matthews, T.K. Maycock, T. Waterfield, O. Yelekçi, R. Yu, B. Zhou (Eds.), Technical Summary. Climate Change 2021: The Physical Science Basis. Contribution of Working Group I to the Sixth Assessment Report of the Intergovernmental Panel on Climate Change, Cambridge University Press, 2021, https://www.ipcc.ch/report/ar6/wg1/.

[30] K. Riahi, D.P. van Vuuren, E. Kriegler, J. Edmonds, B.C. O'Neill, S. Fujimori, N. Bauer, K. Calvin, R. Dellink, O. Fricko, W. Lutz, A. Popp, J.C. Cuaresma, S. KC, M. Leimbach, L. Jiang, T. Kram, S. Rao, J. Emmerling, K. Ebi, T. Hasegawa, P. Havlik, F. Humpenöder, L.A. Da Silva, S. Smith, E. Stehfest, V. Bosetti, J. Eom, D. Gernaat, T. Masui, J. Rogelj, J. Strefler, L. Drouet, V. Krey, G. Luderer, M. Harmsen, K. Takahashi, L. Baumstark, J.C. Doelman, M. Kainuma, Z. Klimont, G. Marangoni, H. Lotze-Campen, M. Obersteiner, A. Tabeau, M. Tavoni, The shared socioeconomic pathways and their energy, land use, and greenhouse gas emissions implications: an overview, Glob. Environ. Change 42 (2017) 153–168, https://doi.org/10.1016/j.gloenvcha.2016.05.009, https://www.sciencedirect.com/science/article/pii/S0959378016300681.

[31] S. Deb, Philos. Mag. 27 (4) (1973) 801–822, https://doi.org/10.1080/14786437308227562, https://www.scopus.com/inward/record.uri?eid=2-s2.0-0015615177&doi=10.1080%2f14786437308227562&partnerID=40&md5=71a51d7cd5e64d20bbb7bf20f31b4a56.

[32] M. Brzezicki, A systematic review of the most recent concepts in smart windows technologies with a focus on electrochromics, Sustainability 13 (17) (Sep 2021), https://doi.org/10.3390/su13179604.

[33] S. Nundy, A. Mesloub, B.M. Alsolami, A. Ghosh, Electrically actuated visible and near-infrared regulating switchable smart window for energy positive building: a review, J. Clean. Prod. 301 (Jun 2021), https://doi.org/10.1016/j.jclepro.2021.126854.

[34] C.G. Granqvist, Electrochromics for smart windows: oxide-based thin films and devices, Thin Solid Films 564 (2014) 1–38, https://doi.org/10.1016/j.tsf.2014.02.002.

[35] C. Gu, A.-B. Jia, Y.-M. Zhang, S.X.-A. Zhang, Emerging electrochromic materials and devices for future displays, Chem. Rev. 122 (2022) 14679–14721, https://doi.org/10.1021/acs.chemrev.1c01055.

[36] Y.-Q. Feng, M.-L. Lv, M. Yang, W.-X. Ma, G. Zhang, Y.-Z. Yu, Y.-Q. Wu, H.-B. Li, D.-Z. Liu, Y.-S. Yang, Application of new energy thermochromic composite thermosensitive materials of smart windows in recent years, Molecules 27 (5) (Mar 2022), https://doi.org/10.3390/molecules27051638.

[37] X. Wang, S. Narayan, Thermochromic materials for smart windows: a state-of-art review, Front. Energy Res. 9 (Dec 2021), https://doi.org/10.3389/fenrg.2021.800382.

[38] M. Aburas, V. Soebarto, T. Williamson, R. Liang, H. Ebendorff-Heidepriem, Y. Wu, Thermochromic smart window technologies for building application: a review, Appl. Energy 255 (Dec 2019), https://doi.org/10.1016/j.apenergy.2019.113522.

[39] M. Kamalisarvestani, R. Saidur, S. Mekhilef, F.S. Javadi, Performance, materials and coating technologies of thermochromic thin films on smart windows, Renew. Sustain. Energy Rev. 26 (2013) 353–364, https://doi.org/10.1016/j.rser.2013.05.038.

[40] D. Moldarev, M.V. Moro, C.C. You, E.M. Baba, S.Z. Karazhanov, M. Wolff, D. Primetzhofer, Yttrium oxyhydrides for photochromic applications: correlating composition and optical response, Phys. Rev. Mater. 2 (11) (Nov 2018), https://doi.org/10.1103/PhysRevMaterials.2.115203.

[41] M.A.A.M. Abdah, H.T.A. Awan, M. Mehar, M.N. Mustafa, R. Walvekar, M.W. Alam, M. Khalid, R. Umapathi, V. Chaudhary, Advancements in mxene-polymer composites for high-performance supercapacitor applications, J. Energy Storage 63 (JUL 2023), https://doi.org/10.1016/j.est.2023.106942.
[42] Y. Zhou, F. Fan, Y. Liu, S. Zhao, Q. Xu, S. Wang, D. Luo, Y. Long, Unconventional smart windows: materials, structures and designs, Nano Energy 90 (B) (Dec 2021), https://doi.org/10.1016/j.nanoen.2021.106613.
[43] Y. Ke, J. Chen, C. Lin, S. Wang, Y. Zhou, J. Yin, P.S. Lee, Y. Long, Smart windows: electro-, thermo-, mechano-, photochromics, and beyond, Adv. Energy Mater. 9 (39) (Oct 2019), https://doi.org/10.1002/aenm.201902066.
[44] W. Shen, G. Li, Recent progress in liquid crystal-based smart windows: materials, structures, and design, Laser Photonics Rev. 17 (1) (JAN 2023), https://doi.org/10.1002/lpor.202200207.
[45] M.S. Castillo, X. Liu, F. Abd-AlHamid, K. Connelly, Y. Wu, Intelligent windows for electricity generation: a technologies review, Build. Simul. 15 (10) (2022) 1747–1773, https://doi.org/10.1007/s12273-022-0895-y.
[46] S. Wu, H. Sun, M. Duan, H. Mao, Y. Wu, H. Zhao, B. Lin, Applications of thermochromic and electrochromic smart windows: materials to buildings, Cell Reports Phys. Sci. 4 (5) (2023) 101370, https://doi.org/10.1016/j.xcrp.2023.101370, https://www.sciencedirect.com/science/article/pii/S2666386423001388.
[47] K. Lin, L. Chao, H.H. Lee, R. Xin, S. Liu, T.C. Ho, B. Huang, K.M. Yu, C.Y. Tso, Potential building energy savings by passive strategies combining daytime radiative coolers and thermochromic smart windows, Case Stud. Therm. Eng. 28 (Dec 2021), https://doi.org/10.1016/j.csite.2021.101517.
[48] S. Xie, Y. Chen, Z. Bi, S. Jia, X. Guo, X. Gao, X. Li, Energy storage smart window with transparent-to-dark electrochromic behavior and improved pseudocapacitive performance, Chem. Eng. J. 370 (2019) 1459–1466, https://doi.org/10.1016/j.cej.2019.03.242.
[49] A. Khatibi, M.H. Jahangir, F.R. Astaraei, Energy and comfort evaluation of a novel hybrid control algorithm for smart electrochromic windows: a simulation study, Sol. Energy 241 (2022) 671–685, https://doi.org/10.1016/j.solener.2022.06.045.
[50] Y. Lin, W. Yang, Solar energy model and thermal performance of an electrochromic dome-covered house, Environ. Sustain. Dev. 39 (2017) 82–90, https://doi.org/10.1016/j.esd.2017.05.001, https://www.sciencedirect.com/science/article/pii/S0973082616305142.
[51] Z. Rashidzadeh, N.H. Matin, A comparative study on smart windows focusing on climate-based energy performance and users' comfort attributes, Sustainability 15 (3) (Feb 2023), https://doi.org/10.3390/su15032294.
[52] H. Fekri, M. Soltani, M. Hosseinpour, W. Alharbi, K. Raahemifar, Energy simulation of residential house integrated with novel iot windows and occupant behavior, Sustain. Cities Soc. 78 (Mar 2022), https://doi.org/10.1016/j.scs.2021.103594.
[53] J. Hoon Lee, J. Jeong, Y. Tae Chae, Optimal control parameter for electrochromic glazing operation in commercial buildings under different climatic conditions, Appl. Energy 260 (2020) 114338, https://doi.org/10.1016/j.apenergy.2019.114338, https://www.sciencedirect.com/science/article/pii/S0306261919320252.
[54] R.F. De Masi, V. Festa, A. Gigante, S. Ruggiero, G.P. Vanoli, The incidence of smart windows in building energy saving and future climate projections, in: 7th International Conference on Advances on Clean Energy Research (ICACER), Barcelona, Spain, Apr 20-22, 2022, Energy Rep. 8 (16) (2022) 283–289, https://doi.org/10.1016/j.egyr.2022.10.222.
[55] D.B. Crawley, L.K. Lawrie, Tmyx weather database, https://climate.onebuilding.org/, 2023.
[56] S. Guillén-Lambea, B. Rodríguez-Soria, J.M. Marín, Air infiltrations and energy demand for residential low energy buildings in warm climates, Renew. Sustain. Energy Rev. 116 (2019) 109469, https://doi.org/10.1016/j.rser.2019.109469, https://www.sciencedirect.com/science/article/pii/S136403211930677X.
[57] EIA, Use of energy explained: energy use in homes [online], https://www.eia.gov/energyexplained/use-of-energy/electricity-use-in-homes.php. (Accessed 9 January 2023), 2015.
[58] Passive house international web-site [online], https://passivehouse-international.org. (Accessed 14 November 2023), 2023.
[59] Energy logic web-site [online], https://theenergylogic.com/blog/major-changes-to-the-2021-residential-iecc/. (Accessed 18 December 2023), 2023.
[60] V.R. Salcido, Y. Chen, Y. Xie, Z.T. Taylor, Cost-effectiveness of the 2021 iecc for residential buildings in New Mexico pnnl-31613, Tech. Rep., Pacific North West National Laboratory, 2021, https://www.energycodes.gov/sites/default/files/2021-07/NewMexicoResidentialCostEffectiveness_2021.pdf.
[61] O.S. Coalition, Open studio coalition website [online], https://openstudiocoalition.org/. (Accessed 9 January 2023), 2023.
[62] Github open studio repository tag for sdk 3.5.1 code [online], https://github.com/NREL/OpenStudio/releases/tag/v3.5.1. (Accessed 29 December 2023), 2022.
[63] EcoDrain, Ecodrain website [online], https://ecodrain.com/en/. (Accessed 9 April 2023), 2023.
[64] G. Dalla Santa, A. Galgaro, R. Sassi, M. Cultrera, P. Scotton, J. Mueller, D. Bertermann, D. Mendrinos, R. Pasquali, R. Perego, S. Pera, E. Di Sipio, G. Cassiani, M. De Carli, A. Bernardi, An updated ground thermal properties database for gshp applications, Geothermics 85 (2020) 101758, https://doi.org/10.1016/j.geothermics.2019.101758, https://www.sciencedirect.com/science/article/pii/S0375650519301944.
[65] A. Roth, D. Goldwasser, A. Parker, There's a measure for that!, Energy Build. 117 (2016) 321–331, https://doi.org/10.1016/j.enbuild.2015.09.056, https://www.sciencedirect.com/science/article/pii/S0378778815302966.
[66] U.S. Department of Energy, Energyplus version 22.2.0 documentation: application guide for energy management system (EMS), https://energyplus.net/assets/nrel_custom/pdfs/pdfs_v22.2.0/EMSApplicationGuide.pdf. (Accessed 13 September 2023), 2022.
[67] R. Dutta, Modeling an electrochromic window using a multi-criteria control strategy, in: 2018 Building Performance Analysis Conference and SimBuild Co-Organized by ASHRAE and IBPSA-USA Chicago, IL September 26-28, 2018, 2018, pp. 1–8, https://www.techstreet.com/atis/standards/modeling-an-electrochromic-window-using-a-multi-criteria-control-strategy?product_id=2026597.
[68] ASHRAE, Ansi/ashrae standard 55-2020 thermal environmental conditions for human occupancy, Tech. Rep., American Society for Heating Refrigeration and Air-Conditioning Engineers, 2020, https://www.techstreet.com/standards/ashrae-55-2020?product_id=2207271.
[69] ASHRAE, Heating, Refrigeration, and Air-conditioning Engineers, © ASHRAE. Provided to the public as part of ASHRAE'S COVID-19 response. Per international copyright law, additional reproduction, distribution, or transmission in either print or digital form is not permitted without ASHRAE's prior written permission, Tech. Rep., American Society for, 2017, https://www.ashrae.org/File%20Library/Technical%20Resources/COVID-19/52_2_2017_COVID-19_20200401.pdf.
[70] F. King, Filterfast.com filter, purify protect, air filter merv 13 specification data sheet [online], https://www.filtersfast.com/prodimages/FF-MERV13-DATASHEET.pdf. (Accessed 9 January 2023), 2023.
[71] E.P. Agency, Website explaining merv ratings [online], https://www.epa.gov/indoor-air-quality-iaq/what-merv-rating. (Accessed 9 January 2023), 2023.
[72] NREL, Open studio hpxml github repository for water heater open studio measure [online], https://github.com/NREL/OpenStudio-HPXML/blob/0f80b93a49bf6111f1b4a27ea9b066ba62f3d5d2/HPXMLtoOpenStudio/resources/waterheater.rb#L502-L515. (Accessed 9 January 2023), 2023.
[73] D.L. Villa, Institutional heat wave analysis by building energy modeling fleet and meter data, Energy Build. 237 (2021) 110774, https://doi.org/10.1016/j.enbuild.2021.110774, https://www.sciencedirect.com/science/article/pii/S037877882100058X.
[74] D.L. Villa, J.P. Carvallo, C. Bianchi, S.H. Lee, Multi-scenario extreme weather simulator application to heat waves, in: Proceeding of the Building Performance Analysis Conference and SimBuild Co-Organized by ASHRAE and IBPSA-USA, 2022, pp. 49–58.
[75] N. Oceanic, A. Association, Global historical climatology network daily (ghcnd) version 3.28-upd-2021100417 [online], https://www.ncei.noaa.gov/data/global-historical-climatology-network-daily/archive/. (Accessed 18 December 2023), 2023.
[76] N. Oceanic, A. Association. U.S. climate normals for 1991-2020 [online], https://www.ncei.noaa.gov/data/normals-hourly/1991-2020/archive/. (Accessed 18 December 2023), 2021.
[77] Y. Dodge, Kolmogorov–Smirnov Test, Springer, New York, New York, NY, 2008, pp. 283–287.
[78] D.L. Villa, S.H. Lee, C. Bianchi, J.P. Carvallo, I. Azaroff, A. Mammoli, T. Schostek, Multi-scenario extreme weather simulator application to heat waves: Ko'olauloa community resilience hub, Sci. Technol. Built Environ. 30 (4) (2024) 375–393, https://doi.org/10.1080/23744731.2023.2279467.
[79] D. Villa, Multi-scenario extreme weather simulator github repository, https://github.com/sandialabs/MEWS, 2023.
[80] E. Lee, M. Yazdanian, S. Selkowitz, The energy-savings potential of electrochromic windows in the us commercial buildings sector, Tech. Rep., Lawrence Berkeley National Laboratory, 2004, https://eta-publications.lbl.gov/sites/default/files/lbnl-54966.pdf.
[81] S.-J. Lee, S.-Y. Song, Energy efficiency, visual comfort, and thermal comfort of suspended particle device smart windows in a residential building: a full-scale experimental study, Energy Build. 298 (2023) 113514, https://doi.org/10.1016/j.enbuild.2023.113514, https://www.sciencedirect.com/science/article/pii/S0378778823007442.
[82] Q. Zhou, F. Xue, Pushing the boundaries of modular-integrated construction: a symmetric skeleton grammar-based multi-objective optimization of passive design for energy savings and daylight autonomy, Energy Build. 296 (2023) 113417, https://doi.org/10.1016/j.enbuild.2023.113417, https://www.sciencedirect.com/science/article/pii/S0378778823006473.
[83] A. Roth, Femy: future and extreme weather data [online], https://www.energy.gov/eere/buildings/femy-future-and-extreme-weather-data.
[84] D. Villa, EnergyPlus Models Github Permalink [online], https://github.com/sandialabs/MEWS/tree/c1a9be57a9e2adf863c373e2823e4b8e470995db/examples/example_data/ClimateZone5B_SantaFe/EnergyPlusModels/09072023.